AD-755 218

DETERMINATION OF ROCK THERMAL PROPERTIES

James F. Bacon, et al

United Aircraft Research Laboratories

Prepared for:

Bureau of Mines
Advanced Research Projects Agency

January 1973

REPORT L-911397-4 January 1973

DETERMINATION OF ROCK THERMAL PROPERTIES

By: J. S. Bacon, S. Russell and J. P. Carstens

United Aircraft Research Laboratories
East Hartford, Connecticut 06108

Sponsored by

ADVANCED RESEARCH PROJECTS AGENCY
ARPA Order No. 1579, Amendment 3
(Program Code 62701D)

U. S. BUREAU OF MINES CONTRACT NO. H0220052

May 24, 1972 to December 22, 1972

Total Amount of Contract: $23,746.00

Principal Investigator: J. P. Carstens (203) 565-7238

Project Scientists: Mr. J. Bacon (Viscosity, Conductivity) (203) 565-5870
Mr. S. Russell (Heat of Vaporization) (203) 565-4949

The views and conclusions contained in this document are those of the authors and should not be interpreted as necessarily representing the official policies, either expressed or implied, of the Advanced Research Projects Agency or the U. S. Government.

62

DOCUMENT CONTROL DATA - R & D

(Security classification of title, body of abstract and indexing annotation must be entered when the overall report is classified)

1. ORIGINATING ACTIVITY (Corporate author)
United Aircraft Research Laboratories
East Hartford, Connecticut 06108

2a. REPORT SECURITY CLASSIFICATION
Unclassified

2b. GROUP

3. REPORT TITLE

Determination of Rock Thermal Properties

4. DESCRIPTIVE NOTES (Type of report and inclusive dates)
Final Report - May 24, 1972 to December 22, 1972

5. AUTHOR(S) (First name, middle initial, last name)

James F. Bacon, Sidney Russell, Jeffrey P. Carstens

6. REPORT DATE
January 1973

7a. TOTAL NO. OF PAGES
56

7b. NO. OF REFS
7

8a. CONTRACT OR GRANT NO.
Bureau of Mines Contract H0220052

b. PROJECT NO.
ARPA Order No. 1579, Amendment 3
(Program Code 627010)

c.

d.

9a. ORIGINATOR'S REPORT NUMBER(S)
L-911397-4

9b. OTHER REPORT NO(S) (Any other numbers that may be assigned this report)

10. DISTRIBUTION STATEMENT

Distribution of this document is unlimited.

11. SUPPLEMENTARY NOTES

12. SPONSORING MILITARY ACTIVITY
ARPA, Dept. of Defense monitored by
Bureau of Mines, Dept. of Interior

13. ABSTRACT

The purpose of this project was to determine, for 10 rock types, the viscosity and electrical conductivity as a function of temperature in the molten state, and the heat of vaporization. The rock types are (1) St. Cloud gray granodiorite (charcoal granite), (2) Westerly granite, (3) Barre granite, (4) Dresser basalt, (5) Sioux quartzite, (6) Berea sandstone, (7) Tholeiitic basalt, (8) Duluth gabbro, (9) Newberry rhyolite, and (10) granodiorite. Viscosity and electrical resistivity measurements were made at temperatures as high as 2200°C, for all rocks except the quartzite. Using the resistivity data, an approximation of the thermal conductivity of the molten rocks was made using the Wiedemann-Franz-Lorenz law, which gives a relationship between the electrical and thermal conductivity. Heat of vaporization of the rocks was measured by vaporizing samples with a CO_2 laser beam. Samples were vaporized in a calorimeter, which measures the partition of input energy among rock heating, rock vaporization, and other losses. For certain rocks, uncontrollable heat losses from the system occur, causing inaccurate determination of heat of vaporization. Suggestions are made on (a) redesign of the experiment to control these losses, and (b) experiments to better identify the heat losses.

DD FORM 1 NOV 65 1473

KEY WORDS	LINK A		LINK B		LINK C	
	ROLE	WT	ROLE	WT	ROLE	WT
Viscosity						
Resistivity						
Heat of Vaporization						
Rock Properties						
Molten Rock Properties						
Thermal Conductivity						
Lasers						
Laser-rock Interaction						

REPORT L-911397-4 January 1973

DETERMINATION OF ROCK THERMAL PROPERTIES

By: J. S. Bacon, S. Russell and J. P. Carstens

United Aircraft Research Laboratories
East Hartford, Connecticut 06108

Sponsored by

ADVANCED RESEARCH PROJECTS AGENCY
ARPA Order No. 1579, Amendment 3
(Program Code 62701D)

U. S. BUREAU OF MINES CONTRACT NO. H0220052

May 24, 1972 to December 22, 1972

Total Amount of Contract: $23,746.00

Principal Investigator:	J. P. Carstens	(203) 565-7238
Project Scientists:	Mr. J. Bacon (Viscosity, Conductivity)	(203) 565-5870
	Mr. S. Russell (Heat of Vaporization)	(203) 565-4949

FOREWORD

The work described in this report was performed at the United Aircraft Research Laboratories, East Hartford, Connecticut, for the Department of the Interior, Bureau of Mines, under Contract No. H0220052. The work was initiated on May 24, 1972 and ended on December 22, 1972.

Participants in this work at UARL included:

J. F. Bacon - Determination of Rock Properties in the Molten State
S. Russell - Measurement of Heat of Vaporization
J. D. Rockenfeller - Measurement of Heat of Vaporization
J. P. Carstens - Program Management

The contracting officer for the work was Mr. Frank Pavlich at the Bureau of Mines in Denver, Colorado. Technical monitoring was provided by Mr. David Lindroth at the U. S. Bureau of Mines Twin Cities Mining Research Center in Minneapolis, Minnesota.

Report L-911397-4

Determination of Rock Thermal Properties

TABLE OF CONTENTS

Report L-911397-4

Determination of Rock Thermal Properties

REPORT SUMMARY

The purpose of the work described in this report is to determine the viscosity and electrical conductivity as a function of temperature in the molten state, and heat of vaporization for ten rock types. The rock types considered are:

1. St. Cloud gray granodiorite (charcoal granite)
2. Westerly granite
3. Barre granite
4. Dresser basalt
5. Sioux (Jasper) quartzite
6. Berea sandstone
7. Tholeiitic basalt
8. Duluth gabbro
9. Newberry rhyolite (fresh)
10. Granodiorite

The viscosity measurements were made using a Brookfield Synchro-Electric Viscometer, a widely-used, standard viscosity measuring device. This viscometer had been previously adapted by the United Aircraft Research Laboratories (UARL) to make viscosity measurements in melts at temperatures up to 2020 °C. Viscosity is determined by the degree of resistance to rotation felt by a cylindrical spindle being rotated in a cup of molten rock. Electrical resistivity was measured using the same furnace, by measuring the resistance between the walls of the tungsten crucible holding the molten rock, and an electrode in the middle of the melt. Viscosity and resistivity data were recorded for all the rock types except the quartzite. The temperature range of molten quartzite is above the temperature capability of the furnace, and no data were taken for that rock type. Measurements were taken successfully, however, on Berea sandstone over a temperature range of from 2090 to 2200 °C.

Using the electrical resistivity data, a first approximation was made to the thermal conductivity of the molten rocks using the Wiedemann-Franz-Lorenz law, which is a simple relationship between electrical conductivity and thermal conductivity which has been used primarily to relate properties of metals. The resulting thermal conductivity values are surprisingly low.

Measurement of heats of vaporization was first attempted by measuring rock vapor pressure as a function of temperature and inferring heat of vaporization from the Clapeyron equation. This method was unusable due primarily to problems

6

encountered in monitoring vapor pressure and vapor species at the temperatures of interest. Also, the use of the data thus generated in analyzing much faster vaporization processes, such as caused by an intense electron beam or laser beam, is questionable. Therefore, an attempt was made to measure the heat of vaporization directly by vaporizing rock with a high-intensity laser beam.

Using this approach, a small sample of rock was placed inside an instrumented calorimeter, and small amounts of rock (of the order of .05 grams) are vaporized directly by a pulse of laser energy added from a hole in the top of the calorimeter. The calorimeter is instrumented to read the amount of heat left in the rock sample, and the amount of heat reflected or reradiated from the sample (except for that amount that radiates directly out of the hole through which the laser energy is admitted). The results show good agreement between the measured total heat of vaporization of quartzite and published values for quartz. However, there are uncontrollably large amounts of heat lost from the system when testing the granites, granodiorites, sandstone and clear quartz test samples. The heat lost in these tests causes a very high and inaccurate indication of heat of vaporization. The heat lost is due either to (a) laser energy reflected directly out of the system from the layer of molten rock created by the laser pulse, (b) laser energy absorbed in a laser energy-initiated plasma shielding the interaction zone, or (c) laser energy reflected from this plasma.

To overcome this problem, the calorimeter can be redesigned to minimize the reflection or reradiation of laser energy from the calorimeter. Such a redesign is suggested, but was not built under this program. To help determine the nature of the energy losses, experiments are suggested to determine the reflection of CO_2 laser radiation from molten rock surfaces at various temperatures of the molten rock.

7

INTRODUCTION

The Bureau of Mines has for years been pursuing a systematic investigation of thermal rock fracture techniques. In recent years this has included consideration of advanced thermal tools, such as electron beams and lasers. In addition to pursuing experimental work, a theoretical understanding of the heat interaction with the rock has also been sought. The extremely intense power density available with electron beams or lasers can cause substantial melting and vaporization of the rock. To theoretically model such interaction, rock thermal properties in the molten state and at vaporization temperatures are required.

The purpose of the work reported on below was to experimentally determine, for a selected set of rocks, the viscosity and electrical conductivity as a function of temperature in the molten state, and the heat of vaporization. In addition, an estimate of thermal conductivity in the molten state was to be made from the conductivity data. Rocks to be studied include:

1. St. Cloud gray granodiorite (charcoal granite)
2. Westerly granite
3. Barre granite
4. Dresser basalt
5. Sioux quartzite
6. Berea sandstone
7. Tholeiitic basalt
8. Duluth gabbro
9. Newberry rhyolite
10. Granodiorite

8

PROPERTY MEASUREMENTS IN THE MOLTEN STATE

Measurement of Viscosity

The viscosity of the molten rocks was measured with a Brookfield Synchro-Electric viscometer from their melting point to a temperature about 300°C above their melting point. Samples were prepared by cutting rock cylinders from the government-furnished rock blocks with a diamond-core drill. (Two such samples were tested of granodiorite, charcoal granite, and Westerly granite; only one sample was tested of each of the other rock types.) The rock cylinders fitted loosely in the thin-wall tungsten crucible, which has a two-inch inside diameter and is three inches high. The tungsten crucible and rock were then placed in a tungsten element furnace as shown in Fig. 1 and heated under vacuum to about 1000°C. At this point, the vacuum was replaced by a 4 psi purified argon atmosphere and the tungsten spindle shown in Fig. 2 was suspended on the central axis of the crucible. Heating was then continued in the argon atmosphere until the rock was molten. At this point the tungsten spindle and attached rod were inserted into the molten rock until the center of the spindle coincided with the center of the crucible. The rod was brought out of the furnace through a special low friction fitting to the Brookfield viscometer used as the measuring mechanism.

This Brookfield Synchro-Electric Viscometer* is a widely used, standard viscosity measuring device. A cylinder or disc or spindle is rotated in the fluid under test through a beryllium-copper spring whose deflection is read on a dial. The dial reading is multiplied by a single constant to obtain the viscosity at the particular rotational speed. When special-design spindles are used, the device is calibrated through the use of oils of known viscosity. Measurements made at different speeds are used to describe the complete flow properties of the material at hand.

The Brookfield viscometer is not customarily used at temperatures as high as those experienced in this work. Therefore, the device was equipped with a special long shaft entering the furnace and with a spindle of suitable high-temperature material. Tungsten was selected as the material for both the spindle and shaft because of its known compatibility with all the molten oxide systems investigated to date. The tungsten spindle (Fig. 2), designed by the Brookfield Engineering Laboratories, and the viscometer were calibrated using the National Bureau of Standards' standard viscosity oil by placing an exact silica replica of the tungsten crucible normally used in the constant temperature bath shown in Fig. 3, filling the silica crucible with oil "P" and running the tungsten spindle in the crucible in such a way as to exactly simulate high-temperature operations. In this manner, the calibration data are obtained for the tungsten spindle as shown graphically in Fig. 4.

*Registered Trademark

The viscosity data were verified by taking the information furnished on the NBS certificate accompanying oil "P", plotting it as shown by the dotted line in Fig. 5, taking the data furnished in the article by Shartsis and Spinner (Ref. 1) and plotting it as the solid line of Fig. 5 to give a displaced similarly-shaped curve. Experience gained in measuring the viscosity of fused silica (Ref. 2) has shown this procedure to be reliable. The complete apparatus is shown in Fig. 6.

To demonstrate repeatability of the viscosity measurements, several tests were made wherein viscosity was measured at a given temperature several times as the sample temperature is cycled up and down. Comparative viscosity measurements generated in this manner are shown in Table I. As shown in the table, the results thus generated could vary by as much as ±18 percent. These data establish the accuracy of repeatability of the measurements. Actual accuracy of the readings can only be checked against some "known" rock viscosity data, which are unavailable.

Limitations on the reading accuracy of the viscometer prevent accurate measurement of viscosity at less than about 80 poises. For this reason, viscosity measurements were not taken at temperatures much beyond the point at which the viscosity falls below 80 poises.

The data obtained on the molten rocks with this device are shown in Figs. 7 through 15. No viscosity data were taken on the Sioux quartzite, since the melting point was above the temperature capability of the system. Specifically, the viscosity of the quartzite at 2200° was above the range of measurement at that temperature (i.e., $\lesssim$ 2600) with the above-described apparatus.

Measurement of Electrical Resistivity

The rock sample to be studied was again prepared by using a diamond-core drill to produce a rock cylinder that loosely fitted the two-inch-wide, three-inch-high, thin-wall tungsten crucible. The crucible and rock were then placed in a tungsten element furnace and heated under vacuum to about 1000°C. At this point, argon was admitted to a pressure of 4 psi and a tungsten ball (1/2-inch-diameter), hung on a thin tungsten rod, was suspended on the central axis of the crucible. Heating was then continued in the argon atmosphere until the rock melted. After melting, the tungsten ball was inserted in the molten rock until it reached the center of the liquid body. The rod supporting the tungsten ball and a rod fastened to the outside of the tungsten crucible were brought out of the furnace through appropriate electrically insulated seals. These rods formed the leads which were connected to the resistance measuring device.

Originally, it was thought that the resistance of the molten rocks might drop to values similar to those found for metals at high temperatures, and a Kelvin double bridge was employed as the measurement device. However, the molten rock resistance was too great to be read on the Kelvin double bridge so a laboratory

model Wheatstone bridge was substituted. The Wheatstone bridge was satisfactory but the measurements were tedious and slow. The instrument finally used was a General Radio Type 1650-A Impedance Bridge, which proved both rapid and accurate. With this bridge the AC resistance of the nine molten rocks at one kilocycle/second was determined as a function of temperature. These data were then converted to specific resistivity and are shown on Figs. 16 through 24.

Errors in the resistivity data could result from errors in temperature measurement or errors in the resistivity measurement at a given point. The accuracy of the impedance bridge is ±1%, as specified in the bridge manufacturer's literature. Large errors in the thermocouple temperature measurement are unlikely, as calibrated thermocouple wire was utilized in their construction. However, it is possible that the errors in the reproducibility of the viscosity data could be all due to the thermocouples, in which case the same range of error could exist in the resistivity data. On this basis, the accuracy of the resistivity data may be conservatively estimated to be ±18%.

Approximate Prediction of Thermal Conductivity of Molten Rocks

The measurement of thermal conductivity, especially of a molten material at high temperatures, is slow and expensive. On the other hand, the measurement of the electrical conductivity of a liquid at high temperatures is relatively simple, cheap and rapid. In 1853, Wiedemann & Franz formulated an empirical law relating the thermal conductivity and electrical conductivity which stated that the ratio of these two conductivities for a metal are a constant for all metals. In 1872, Lorenz discovered that the Wiedemann-Franz ratio is proportional to temperature and the result was the Wiedemann-Franz-Lorenz law stating

$$\frac{K}{\sigma} = K\rho = LT$$

where σ = electrical conductivity
ρ = electrical resistivity
T = absolute temperature
L = Lorenz number
K = the thermal conductivity

This relationship can readily be derived from Boltzmann statistics as well as from quantum statistics. It is accurate for metals at temperatures well above the Debye temperatures and where the electronic conductivity is considerably larger than the lattice conductivity. As a rock is melted, its electrical resistivity rapidly decreases and any lattice conductivity it may possess is largely destroyed. This phenomenon has been employed to predict the thermal conductivity of metallic alloys at normal temperatures (Ref. 3).

11

For the present case, a theoretical prediction of the thermal conductivity of the molten rock is made, based on the assumption that the electrical conductivity and thermal conductivity of the magma are largely electronic in nature at these very high temperatures. The results of the calculations are tabulated in Table II and must be regarded only as a first approximation until confirmed by actual measurement of the thermal conductivity.

Although a small thermal conductivity is predicted for amorphous solids or molten liquids since the mean free path of the phonons is approximately constant at short wavelengths and the long wavelengths are not scattered so effectively, the fact that such low values of thermal conductivity are found (Table II) is still surprising and indicates the need for further research.

HEAT OF VAPORIZATION MEASUREMENTS

Heat of Vaporization from Clapeyron Equation

An attempt was made to determine heats of vaporization by measuring rock vapor pressure as a function of temperature, and deriving the heat of vaporization from the Clapeyron equation. After several attempts to generate the necessary experimental data, it was determined that this approach would not yield the necessary information for the following reasons:

1. The UARL isoteniscope test facility available could not be adapted for accurate vapor pressure measurement due to vapor condensation in the system.

2. Container materials and reliable temperature measuring devices were not available for operation in the temperature range required.

3. Procedures and equipment for determining the constituents of the vapor phase were not available. This shortcoming also prevented use of alternate effusion or transpiration methods of estimating heat of vaporization from vapor pressure data.

4. The stepwise application of heat, as would be used in any conventional vapor pressure measuring technique, is expected to lead to fractional vaporization in the multicomponent rock systems. Thus, the results would not readily correspond to vaporization energy requirements per unit of typical volume of the rock samples, and consequently the results would have limited application to analysis of very high heat-rate rock fracture devices, such as lasers or electron beams.

An alternate technique was therefore pursued to measure rock vaporization energies directly by vaporizing small amounts of rock with a high-power laser pulse.

Heat of Vaporization from Laser Vaporization Tests

In this technique, a high quality laser beam is used to vaporize a portion of a rock sample, within a system which is instrumented to allow monitoring of the energy partition of the input laser pulse among vaporization of the rock, heating of the rock, heating of the container, etc. The heat of vaporization is then determined directly from the weight of material vaporized, and the measured heat energy associated with the vaporization process. This approach has several basic advantages over the vapor pressure measurement approach. For one thing, since the high-energy laser pulse completely vaporizes a small volume of the rock sample, the problem of fractional vaporization of various rock components is avoided. Thus, a

breakdown and knowledge of the molecular weights for the various vaporized species is not required as it is in the conventional method. Also, since only a localized section of the rock sample is intensively heated, the rock sample acts as its own container for the vaporization experiment. Therefore, the rest of the system remains comparatively cool, allowing the use of conventional materials for holders, shields, and other system components. Finally, the simplicity of the approach and the apparatus allows an extensive amount of data to be taken in a relatively short time and for relatively small cost, once the apparatus is fabricated and appropriately calibrated.

Test Apparatus and Test Procedures

A sketch of the "laser vaporization" test apparatus is shown in Fig. 25. The laser beam (B) enters through a small port (P) at the top whence, after being defocused slightly, it strikes the test sample (S). The test sample is contained in a small copper cup (H) that is supported by a quick release mechanism (M) so that cup and test sample may be quickly dropped into a dry calorimeter (D). The dry calorimeter consists of a glass sleeve (G) with a thin-walled copper end cap (E) cemented at the bottom. The end cap is immersed in a small volume of water contained within an evacuated thermos flask (F). Provisions for stirring and monitoring the temperature of the water are present. The cup and test samples, while supported in the quick release mechanism, are surrounded by a thin-walled copper cone (C) which is instrumented for temperature measurements. This shield is blackened on the inside with a light coating of carbon soot and serves to capture heat deflected or otherwise lost from the truncated sample surface. It also serves as a site on which the rock vapors might condense. The sleeve is readily removable from its supporting collar (R) for weighing as part of each test. Another thin-walled copper sleeve (L) lines most of the inner wall of the glass sleeve. It is blackened also and instrumented for temperature measurements. It serves to monitor any stray heat losses. At the top of the apparatus a gas port (A) is provided in order to permit a sweep of the test sample environment with argon gas before each test.

The assembled apparatus is shown in Fig. 26. It is shown disassembled in Fig. 27. The removable elements, i.e., the specimen holder, specimen, shield, and liner (left to right), are shown in Fig. 28.

The laser beam is aimed from above. Final alignment of the high-energy laser beam with respect to the sample target is made with the aid of an auxiliary helium-neon laser beam. This alignment is facilitated by having the test apparatus mounted on a stage which is movable in all directions. The diameter of the high-energy beam that will strike the sample is controlled by the distance the stage is moved beyond the focal point of the beam. For all tests, the rock surface was located sufficiently far from the focal point to allow a beam "spot size" of the order of 1/8 inch. The duration of the laser pulse is controlled by a mechanically

operated shutter. The power level is measured and set using well-tested calorimeters which are integral with the laser unit used. During these tests the power was varied between .05 and 4.0 kilowatts. The wavelength of the beam was 10.6μ.

The following test procedure was followed. The sample (S), sample holder (H), blackened cone (C), and blackened liner (L) are preweighed and installed in the test apparatus. A small measured volume of water is added to the thermos. Final beam alignment adjustments are made using the helium-neon beam and sighting through mirrors to assure that the high-energy beam will strike the sample properly. The water stirrer is turned on. The sample environment is flushed with argon for about 30 seconds. Then, with all temperature recorders on, the high-energy beam is pulsed in using a preselected shutter speed. The sample and sample holder are then immediately released into the dry calorimeter. All system temperature changes are recorded. As would be expected from the poor heat conductivity of the sample, the slowest response is found in the dry calorimeter, where it takes from three to five minutes for the temperature to stabilize. The other temperatures stabilize almost immediately.

The sample, sample holder, shield and liner are retrieved and reweighed. The water is drained from the thermos and replaced with fresh water at room temperature. A new set of sample, sample holder, shield and liner is installed for the next test run.

Data Reduction

The energy that enters the calorimeter system shown in Fig. 25 is either absorbed by the rock sample or reflected from the rock either (a) into the heat shield assembly or (b) out of the hole at the top of the calorimeter. Of the energy absorbed by the rock, some of this is expended in vaporizing the rock, and the rock vapors may then either condense within the calorimeter or be carried out of the system. Additional heat losses can be due to heat lost from the system by convection from the shield or rock sample either during the laser pulse or after the pulse when the system is coming to equilibrium. Thus:

$$H_{input} = H_{rock} + H_{shield} + H_{argon} + H_{liner} + H_{loss} \qquad (1)$$

The final heat content in the rock is measured by the temperature change in the dry calorimeter, as measured by the maximum temperature of the water bath. This temperature change is applied to the entire rock-holding system, as indicated in Eq. (2):

$$H_{rock} = H_{water} + H_{copper\ end\ cap} + H_{rock\ sample} + H_{rock\ sample\ holder} \qquad (2)$$

15

The final heat content of the shield assembly is determined from the average temperature change of the shield as sensed by thermocouples positioned at various points on the shield.

$$H_{shield} = H_{cone} + H_{collar} \tag{3}$$

In a similar manner, the heat deposited in the shield liner and the argon blanket are calculated from their temperature rise.

Finally, as discussed above, the heat lost from the system may be described as

$$H_{loss} = (Cp\Delta T + H_f + H_v)(W_v - W_c) + H_{refl.} + H_{other} \tag{4}$$

where $\Delta T = T_{vaporization} - T_{room}$

H_f = Heat of fusion

H_v = Heat of vaporization

Cp = Average specific heat of rock between room temperature and vaporization temperature

W_v = Weight of rock vaporized (= weight loss of sample, assumes negligible amount of rock vapors condensed on sample)

W_c = Weight of rock condensing on parts of calorimeter (measured)

$H_{refl.}$ = Laser pulse energy reflected out of top of calorimeter cone during rock-heating

H_{other} = Other losses from the system due to convection or radiation from cone or sample during heating or cooling

All of the terms in Eqs. (2) and (3) are measured during the experiment. H_{input} is known from the laser beam power and pulse time. In Eq. (4), W_v and W_c are measured, and Cp, ΔT and H_f must be known to predict H_v. $H_{refl.}$ and H_{other} are not monitored, and must be small relative to H_{loss} if the method is to be accurate.

Equation (1) may be solved for H_{loss} (since all other terms are known by direct measurement), and this value substituted for the left-hand side of Eq. (4), which may then be solved for H_v. The result of these manipulations gives:

$$H_v = \frac{(H_{input} - \Sigma H_{measured}) - (H_{refl.} + H_{other})}{(W_v - W_c)} - (Cp\Delta T + H_f) \tag{5}$$

where $\Sigma H_{measured} = H_{rock} + H_{shield} + H_{liner} + H_{argon}$.

16

It should be noted that this presumes an identity between the heat of vaporization and the heat of condensation, and also neglects the possibility of any superheating of the rock vapor. Equation (5) also implies that the condensed rock, which is caught in the system, is chemically similar to the volume of rock initially vaporized.

Test Results

A preliminary series of tests was run on quartz to determine the effect of power level and pulse time on the system heat balance. The laser power level was varied between 200 and 2800 watts, and the pulse time varied from 0.5 to 60 seconds. The tests indicated that the amount of sample vaporized per unit of input energy was maximized by using short pulses (0.5 sec was the shortest pulse used). This trend is shown by the data in Fig. 29. The heat inputs to the rock system and the shield are given in Figs. 30 and 31, respectively.

Based on this preliminary test series, test conditions were chosen at which vaporization tests were run for quartz and for each of the ten rock types of interest. The amount of rock material vaporized, the weight of material condensed in the system, and the heat distribution in the system, are listed in Table III.

Values for heat capacity used in calculating heat contents of samples and copper elements are shown in Table IV . Values for quartz were derived from Kelley (Ref. 4). Values obtained by Lindroth, et al (Ref. 5), for Jasper quartzite were used for Sioux quartzite. A mean average of the values for quartz and the Jasper quartzite was used in estimating values for Berea sandstone. Values obtained also from Lindroth, et al, for Dresser basalt were used directly. These same values were applied to tholeiitic basalt. Values used for Westerly granite, Barre granite, granodiorite, St. Cloud granodiorite, and Newberry rhyolite were based upon a mean average of data for Rockville granite and charcoal gray granite also taken from Lindroth, et al. Values used for Duluth gabbro were similar to those used for the basalt materials. Heat contents of all H_{rock} components were determined using values for 25°C. Heat contents of H_{shield} elements were determined using the appropriate value for the final temperature. A value for quartz at vaporization temperature was extrapolated from handbook data.

For the quartz specimen in column 1 of Table III, using Eq. (5) (assuming $H_{loss} = 0$), with the following constants:

$$C_p = .325 \text{ cal/gm } ^\circ\text{C}$$
$$T_{vap} = 2500^\circ\text{C}$$
$$H_f = 33 \text{ cal/gm}$$

The heat of vaporization is 9,722 cal/gm. This compares with a calculated value for H_v of 1400 cal/gm, based on vapor pressure data given in Ref. 6, and using the

17

Clapeyron equation. This indicates that about 113 calories of heat must have been lost from the system. However, for the pure quartzite case (column 5 of Table III) the calculated value of H_V (using Eq. (5)) is 1247 cal/gm (assuming $H_{loss} = 0$), which agrees quite well with the 1400 cal/gm figure. Calculations of H_V for the other ten rock types were not made due to lack of data on average Cp and vaporization temperature, T_V.

However, it is interesting to observe the measured total heat of vaporization, assuming no losses in the system, as calculated from the data in Table III. This calculation is shown in Fig. 32. The calculated total heats of the rocks vary from just under 2,000 cal/gm for tholeiitic basalt to approximately 9,680 cal/gm for the St. Cloud granodiorite. These values can be compared to a theoretical total heat of vaporization of 2148 cal/gm for quartz, as mentioned above. Also shown in Fig. 32 is the amount of material vaporized in each test, which does not exactly correlate with the increase of the measured total heat of vaporization.

It is interesting to note the large difference among the H_{VT} of pure quartz, quartzite, and sandstone, all of which consist mostly or all of SiO_2. This difference cannot be explained, other than to note that differences in surface reflectivity and/or plasma formation and shielding, and hence heat lost from the system, may have existed. With this uncertainty, the accuracy of the values presented for H_{VT} in Fig. 32 cannot be specified other than to say that the values are probably within a factor of 10 of their true amounts. The ordering shown in Fig. 32 may be considered a first approximation to the proper ranking of these rocks with respect to their total heats of vaporization.

Additional Tests with Quartz

The large apparent heat loss from the quartz experiment in column 1 of Table III may have been caused by reflectivity of laser energy from the sample out the top of the hole. If the problem were reflectivity of the molten surface, this could perhaps be modified by introducing different specimen surface shapes. Therefore, several runs were made using differently-shaped specimens. Some of these are shown in Fig. 33. They are shown diagrammatically in Fig. 34. Truncated specimens were used in attempts to control the direction of laser beam deflection. A deep cylindrical hole and a funnel-shaped hole were used in attempts to trap the reflected energy. In all these cases considerable energy loss from the sample persisted, as indicated by the white ray exiting upwards out the throat of the shield. Also, in all cases the vaporized hole patterns were similar.

In order to study the phenomenon further, the laser beam was directed at a number of very low angles of attack onto the side of a quartz specimen suspended in the open so that the deflected path of the beam might be continuously observed. The results of one of these tests are diagrammatically illustrated in Fig. 35. The beam is initially reflected downward. As a hole is vaporized in the specimen, the

direction of the very strong white light changes from downward to straight upwards. The lower the angle of attack, the longer it took for the angle of the white light to change. Noteworthy, at the same time, greater amounts of sample were vaporized.

It was the short-range objective of the above experiments to determine how the test apparatus might be modified to bring the system heat loss under control and to better elucidate the phenomenon.

It is evident that several apparatus design changes would be necessary in order to bring heat losses under greater control and thereby provide for more accurate values for heats of vaporization. These changes would allow a very low angle of attack on the specimen, and controlled capture of lost energy. This could be accomplished in an apparatus of a design such as shown in Fig. 36. In this design, the external cone-shaped calorimeter and the sample holder are water-filled (details not shown). The shield is not water-jacketed but it might be if this later proved desirable.

Relative to the phenomenon of heat loss, it is unclear how much of the heat lost from the system is due to actual reflection off the molten surface, and how much is due to energy absorption in or reflection by a surface-shielding plasma plume. Reference 7 indicates that the reflection of energy at 10.6μ off solid quartz is less than 20%. However, it is possible that the reflectivity of quartz could change in the molten state relative to the solid state. Also, an increase in direct reflectivity could most easily cause energy to be lost from the system out of the top entrance cone. On the other hand, the strong white light observed in the tests, and the increased material vaporization rate at low laser beam angles to the sample, suggest the presence of a radiating plasma.

The above tests are insufficient to determine the relative importance of the different loss modes. In the future, experiments to determine the reflectivity of molten rock at different temperatures could help explain the situation. These tests could involve measurement of a low-power laser beam reflected off a molten rock puddle uniformly heated by nonlaser means (such as the furnace used in the present viscosity experiments) to different temperatures.

CONCLUSIONS

1. Viscosity and electrical conductivity of the molten phase of nine of the ten test rocks are determined. The melting point of the tenth rock type, Sioux quartzite, is too high to allow these measurements. A first approximation to the thermal conductivity in the molten state, based on the electrical resistivity, gives surprisingly low values.

2. Conventional means for evaluating vaporization energies by determining vapor pressure-temperature relationships using isoteniscope, effusion, or transpiration methods, and then deriving a value for heat of vaporization from the Clapeyron equation, have been deemed unsuitable for rock. This is primarily due to problems caused by partial vaporization of components of the nonhomogenous rock mixture which cause (a) problems in monitoring vapor pressures and species, and (b) difficulties in applying the results to rapid vaporization of rocks by electron beams or lasers.

3. A direct measurement of vaporization energy by flash vaporizing a section of rock sample using a known energy input by a laser beam and determining the amount of rock vaporized and the residual heat in the rock was not possible because a sizable (but unspecified) portion of the total energy from the laser was not absorbed by the rock, and accurate values for average rock specific heats and vaporization temperatures are not known.

4. The present method could be used for measuring total vaporization energies if the input energy not absorbed by the sample could be measured in the experimental device. A concept for a calorimeter which might achieve such measurement is presented.

REFERENCES

1. Shartsis, L. and S. Spinner: Viscosity and Density of Optical Glasses. Journal of Research of the National Bureau of Standards, Vol. 56, No. 3, March 1951.

2. Bacon, J. F., et al: Viscosity and Density of Molten Silica and High Silica Content Glasses. Physics & Chemistry of Glasses, Vol. 1, No. 3, June 1960, pp. 90-98.

3. Hust, J. G. and A. F. Clark: The Lorenz Ratio as a Tool for Predicting the Thermal Conductivity of Metals and Alloys. Materials Research and Standards, August 1971.

4. Kelley: U. S. Bureau of Mines Bulletin 584, 1960.

5. Lindroth, D. P. and W. G. Krawza: Heat Content and Specific Heat of Six Rock Types at Temperatures to 1000°C. Bureau of Mines Report of Investigations RI 7503, April 1971.

6. Kelley: U. S. Bureau of Mines Bulletin 383, 1935.

7. Hovis, W. A. and W. R. Callahan: Infrared Reflectance Spectra of Igneous Rocks, Tufts and Red Sandstone from 0.5 to 22μ. Journal of the Optical Society of America, Vol. 56, No. 5, May 1966.

21

TABLE I

REPRODUCIBILITY OF VISCOSITY DATA

Rock Type	Temperature	Viscosity in Poises*	Average Viscosity	Variation in Viscosity Measurements Low	High
Duluth Gabbro	1250 °C	190,193,190,200,215	197.6	4.0 %	8.81%
	1200 °C	790,775,810	791.7	.2 %	2.32%
Westerly Granite	1564 °C	1106,1040,1000	1048.7	4.87%	5.47%
	1583 °C	850,800,800	816.7	2.08%	4.08%
	1695 °C	170,200,235	201.7	18.6%	16.5 %
	1650 °C	650,620,575	615.0	6.97%	5.69%
Charcoal Granite	1674 °C	145,140,145,144.5,145	143.9	2.79%	.76%
	1417 °C	1250,1275,1130,1220	1218.75	7.85%	2.56%
	1540 °C	340,375,383	366.0	7.65%	4.64%
Granodiorite-Lunar	1583 °C	1250,1130,1010	1130.0	11.88%	10.62%
	1706 °C	300,325,250	291.667	16.67%	11.43%
Tholeiitic Basalt	1244 °C	200,230,200,206	209.0	4.5 %	10.05%
	1282 °C	160,164,161.5	161.833	1.15%	1.34%
Altered Rhyolite	1840 °C	837,820,845	834.0	1.71%	1.32%
	1879 °C	700,700,707	702.33	.33%	.66%

*Viscosity measured at different points in heating cycle where the temperature is the same.

TABLE II

ESTIMATED THERMAL CONDUCTIVITY OF TEST ROCKS

Temp. in °Kelvin
K = thermal conductivity in cal. cm/sec °C cm^2

Barre Granite		Westerly Granite		Duluth Gabbro		Charcoal Granite		Granodiorite Lunar		Tholeiitic Basalt		Newberry Rhyolite		Dresser Basalt		Berea Sandstone	
Temp.	K	Temp.	K	Temp.	K	Temp.	K	Temp.	K	Temp.	K	Temp.	K	Temp.	K	Temp.	K
1493	$3.82 \cdot 10^{-6}$	1513	$1.267 \cdot 10^{-5}$	1479	$3.95 \cdot 10^{-7}$	1603	$6.844 \cdot 10^{-6}$	1673	$2.668 \cdot 10^{-5}$	1512	$1.291 \cdot 10^{-5}$	1779	$1.232 \cdot 10^{-5}$	1463	$1.75 \cdot 10^{-5}$	2251	$2.136 \cdot 10^{-6}$
1539	4.29	1513	1.337	15	4.887	1626	8.33			1537	1.788	1884	1.687	1484	2.055	2263	2.366
1561	4.65	1501	1.326	1531	5.447	1653	8.82	1707	1.702	1581	2.250	1873	2.399	1492	2.135	2295	2.556
1693	5.23	1544	1.465	1553	5.94	1695	10.59	1749	1.948	1633	2.988	1892	3.029	1509	2.355	2325	2.905
1625	5.78	1573	1.679	1580	6.979	1735	12.01	1781	2.142	1673	3.571	1931	7.061	1526	2.572	2345	3.47
1647	6.21	1617	1.954	1611	7.787	1773	13.76	1793	2.297	1705	3.798	1979	11.266	1558	3.168	2361	3.877
1696	7.24	1615	1.970	1651	8.999	1792	14.57	1843	2.638	1736	4.447	1998	11.374	1581	3.682	2404	4.967
1716	8.45	1587	1.890	1679	9.775	1807	15.69	1895	3.034			2034	23.684	1607	4.288	2438	6.246
1747	9.73	1601	1.953	1701	10.5	1817	16.62	1923	3.351			2060	23.987	1629	4.742		
1785	11.43	1646	2.108	1728	11.67	1852	18.98					2088	24.313	1657	5.442		
1815	13.68	1683	2.395	1771	12.1	1863	19.89							1683	6.340		
1855	14.85	1703	2.493	1793	12.4	1893	22.04							1706	6.623		
		1731	2.534	1811	12.54									1739	7.425		
		1770	2.834											1777	8.130		
		1815	3.0997											1793	8.538		

TABLE III

SUMMARY OF TESTS ON TEN ROCK SAMPLES

Laser Power Level = 2.8 kw Pulse Time = 0.5 sec

RUN # MATERIAL	1 QUARTZ (CONTROL)	2 WESTERLY GRANITE	3 BARRE GRANITE	4 DRESSER BASALT	5 SIOUX QUARTZITE	6 BEREA SANDSTONE	7 THOLEIITIC BASALT	8 DULUTH GABBRO	9 GRANO-DIORITE	10 ST CLOUD GRANODIORITE	11 NEWBERRY RHYOLITE
H_{input}, calories	327	327	327	327	327	340	327	327	327	327	327
Wt. sample vaporized, g	.02673	.05342	.05012	.08742	.09901	.04528	.07572	.07110	.05420	.05070	.05790
Wt. condensate on shield, g	.01305	.03416	.02527	.02486	.01780	.02299	.02540	.01729	.02910	.03561	.02957
H_{rock}, calories											
H calorimeter water	99.200	65.000	92.5 [illegible]	77.500	82.500	67.500	95.000	90.000	87.500	57.500	62.500
copper end cap (E)	.770	.498	.708	.593	.632	.517	.727	.689	.670	.440	.478
H sample (S)	4.280	3.921	4.992	6.230	3.960	2.330	5.260	5.275	4.701	2.717	2.631
H sample holder (H)	2.900	1.965	2.788	2.334	2.488	2.011	2.896	2.697	2.647	1.730	1.850
SUBTOTAL	107.150	71.384	100.988	86.657	89.580	72.358	103.883	98.661	95.518	62.387	67.459
$H_{shield\ assembly}$, calories											
H cone (C)	51.200	97.100	96.000	72.500	59.000	101.200	105.800	95.400	79.600	95.800	90.800
H collar (R)	7.050	13.290	13.300	10.100	8.280	14.150	14.920	13.510	11.150	13.550	12.600
H copper liner (L)	20.400	6.447	6.317	6.314	6.400	6.490	6.393	6.367	6.230	6.412	6.399
H condensate on shield	.180	.925	.589	.531	.271	.650	.770	.405	.573	.840	.779
H argon blanket	2.000	1.500	1.500	1.500	1.500	1.500	1.500	1.500	1.500	1.500	1.500
SUBTOTAL	81.102	120.502	118.626	91.635	75.853	124.880	130.413	117.822	100.010	119.422	113.098
TOTAL: $H_{rock} + H_{shield\ assembly}$	188.252	191.886	219.614	178.292	165.433	197.238	234.296	216.483	195.528	181.809	180.557
H_{loss}, calories	138.748	135.114	107.386	148.708	161.567	142.762	92.704	110.517	131.472	145.191	146.443

TABLE IV

SPECIFIC HEAT VALUES*

Specific Heat in cal/g °C

MATERIAL / TEMPERATURE, °C	25	100	300	625	900	1500	2200
QUARTZ	.198	.213	.250	.267	.275	.299	.311
SIOUX QUARTZITE	.203	.219	.259	.291	.285	-	-
BEREA SANDSTONE	.200	.216	.254	.279	.280	-	-
DRESSER BASALT	.224	.230	.255	.257	.256	-	-
THOLEIITIC BASALT	.224	.230	.255	.257	.256	-	-
WESTERLY GRANITE	.212	.222	.248	.265	.282	-	-
BARRE GRANITE	.212	.222	.248	.265	.282	-	-
GRANODIORITE	.212	.222	.248	.265	.282	-	-
ST. CLOUD GRANODIORITE	.212	.222	.248	.265	.282	-	-
NEWBERRY RHYOLITE	.212	.222	.248	.265	.282	-	-
DULUTH GABBRO	.224	.230	.255	.257	.256	-	-

*Values for quartz from Kelley, Bureau of Mines Bulletin 584, 1960. Values for Dresser basalt from Lindroth, et al. Bureau of Mines Report of Investigations RI 7503, April 1971. All other values estimated from values reported for similar materials by Lindroth, et al, same reference.

FIG. 1

HIGH TEMPERATURE TUNGSTEN RESISTANCE FURNACE

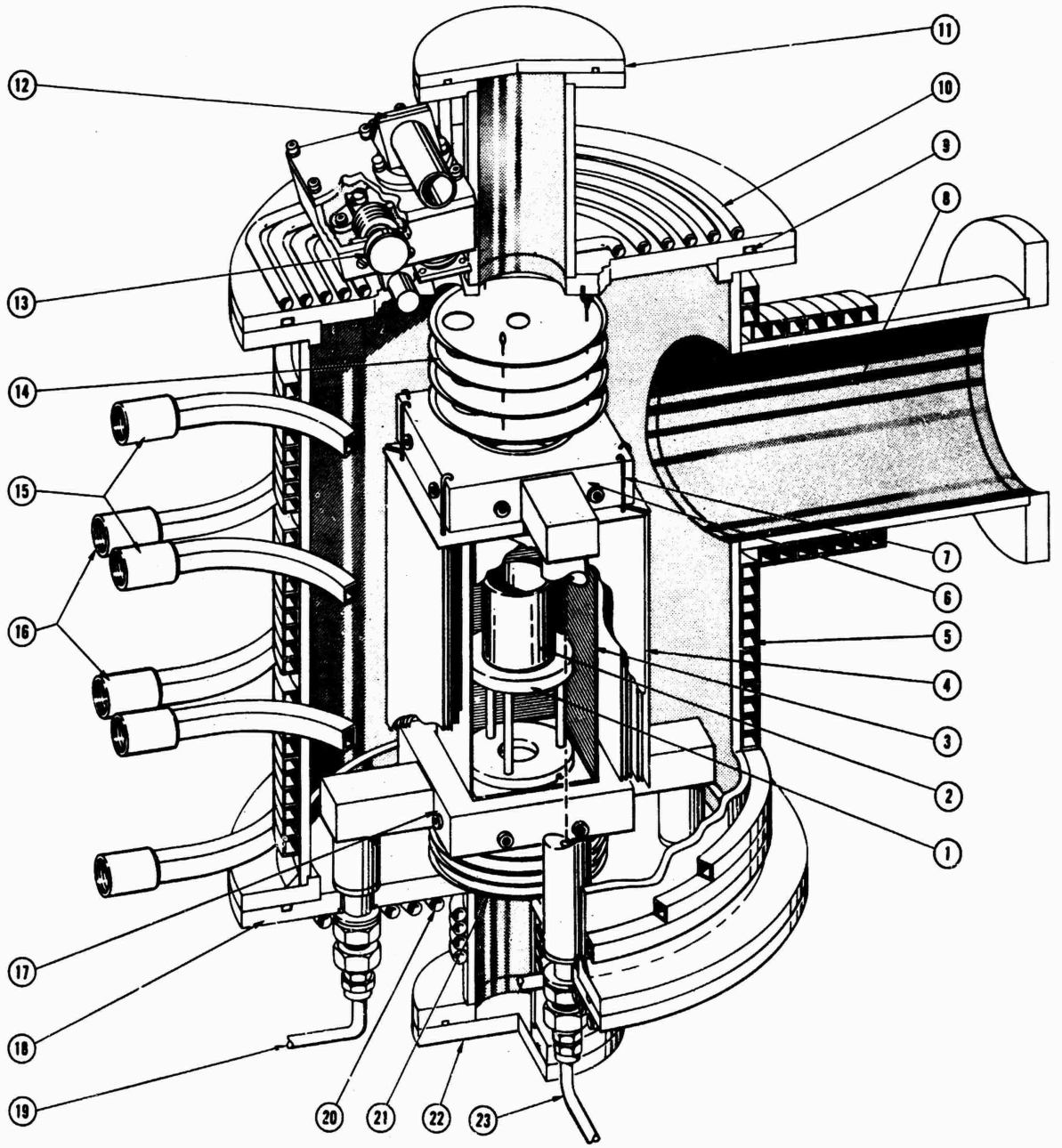

1. TUNGSTEN PEDESTAL FOR CRUCIBLE
2. TUNGSTEN CRUCIBLE
3. FLAT TUNGSTEN HEATING ELEMENT (4)
4. TANTALUM RADIATION SHIELDS
5. SIDE COPPER COOLING COILS
6. TOP WATER COOLED ELECTRODE SUPPORT CONDUCTOR
7. SUPPORT PIN FOR TANTALUM SHIELDS
8. TO VACUUM SYSTEM
9. "O" RING GASKET SEALS
10. TOP COPPER COOLING COILS
11. TOP INTERCHANGABLE COVER FOR MEASURING APPARATUS
12. SIGHT GLASS
13. PROTECTOR MECHANISM FOR SIGHT GLASS
14. TOP TANTALUM RADIATION SHIELDS
15. COOLING WATER IN
16. COOLING WATER OUT
17. BOTTOM WATER COOLED ELECTRODE SUPPORT CONDUCTOR
18. BOTTOM PLATE FOR MOUNTING
19. WATER IN BOTTOM ELECTRODE
20. BOTTOM COPPER COOLING COILS
21. BOTTOM TANTALUM RADIATION SHIELDS
22. BOTTOM INTERCHANGABLE COVER FOR MEASURING APPARATUS
23. WATER IN TOP ELECTRODE

RL-60-178

LARGE TUNGSTEN SPINDLE USED FOR HIGH TEMPERATURE VISCOSITY MEASUREMENT

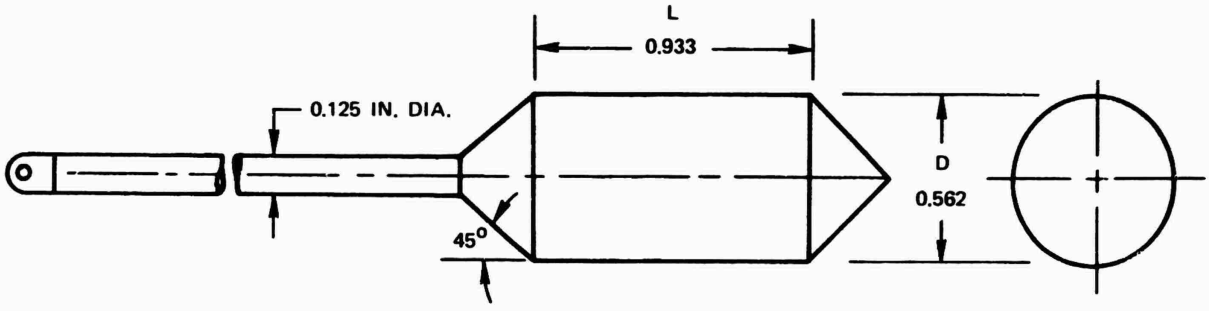

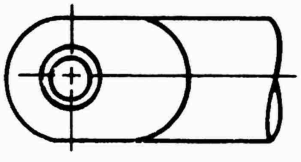

BROOKFIELD VISCOMETER MODEL: RVT

CONTAINER DIAMER: 2 IN.

MINIMUM CONTAINER DEPTH: 2 IN.

SPEED (R.P.M.)	RANGE (CPS)
100	0 – 3000
50	6000
20	15,000
10	30,000
5	60,000
2.5	120,000
1	150,000
0.5	600,000

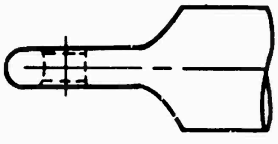

FIG. 3

BROOKFIELD VISCOMETER AND CONSTANT TEMPERATURE BATH USED FOR CALIBRATION

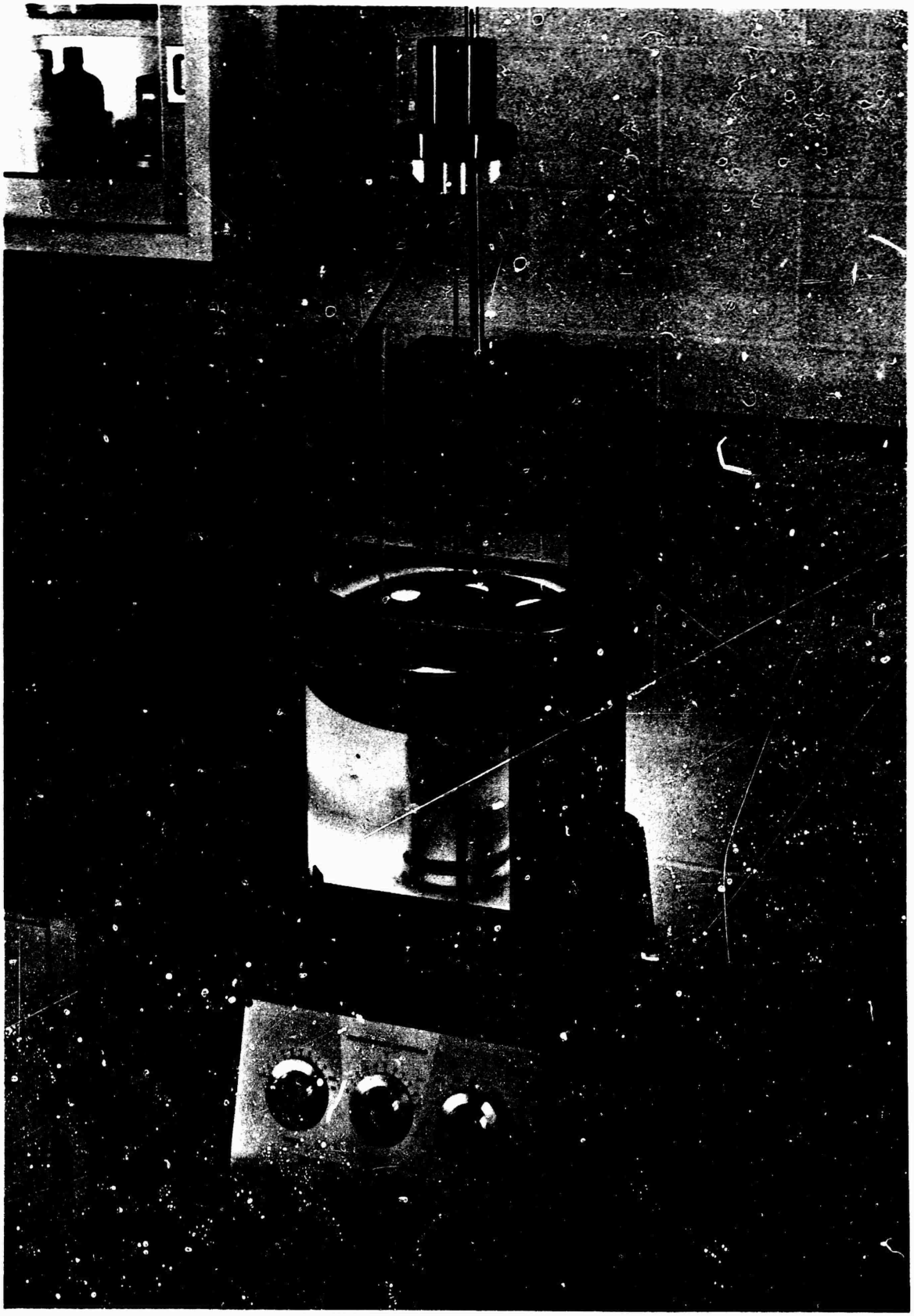

FIG. 4

CALIBRATION DATA FOR LARGE TUNGSTEN SPINDLE, BROOKFIELD VISCOMETER, AND STANDARD OIL "P" FROM N.B.S.

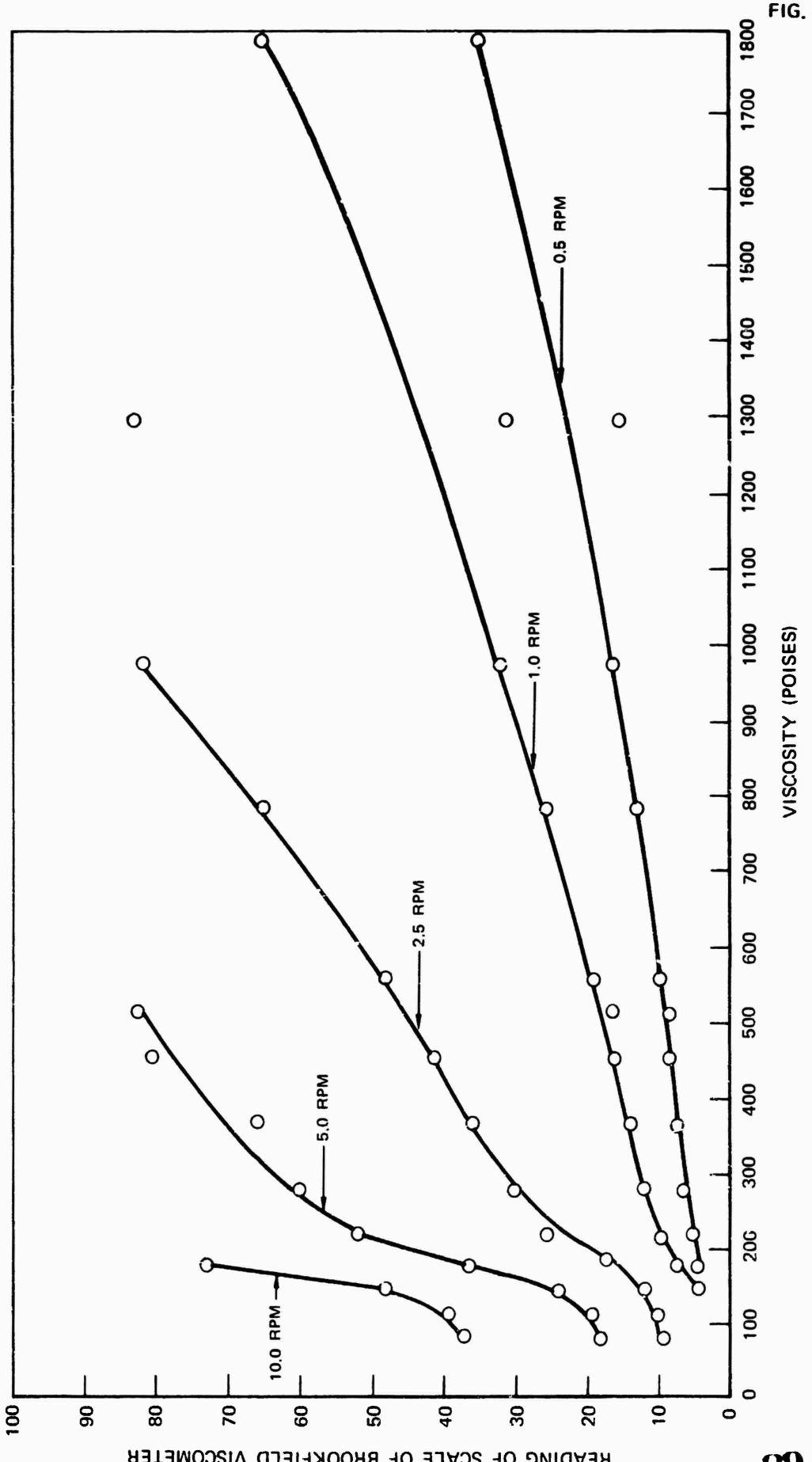

FIG. 5

EXTRAPOLATED CALIBRATION CURVE FOR N.B.S. VISCOSITY STANDARD "P"

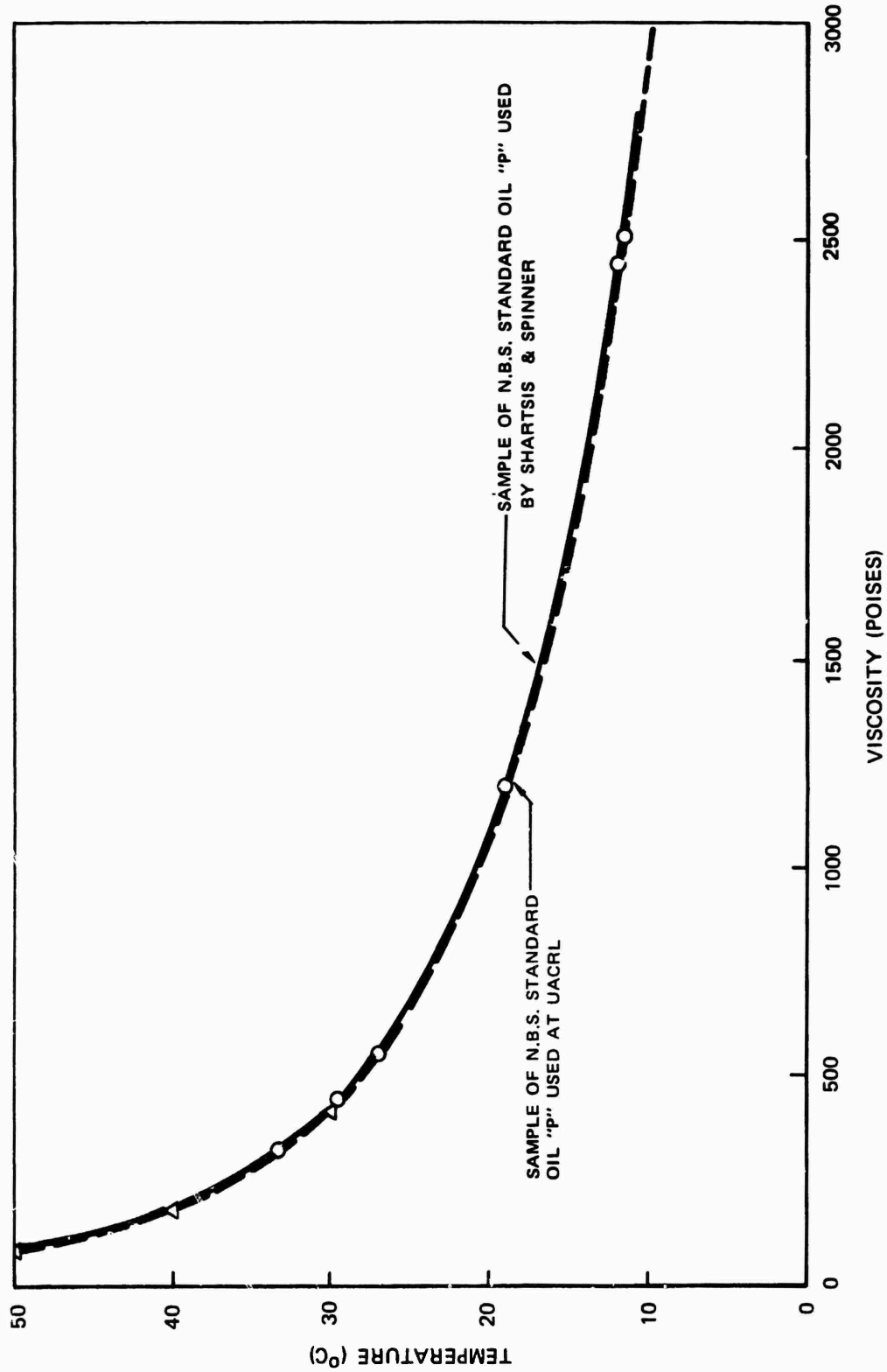

FIG. 6

BROOKFIELD VISCOMETER INSTALLED ON TUNGSTEN FURNACE
FOR HIGH TEMPERATURE VISCOSITY MEASUREMENTS

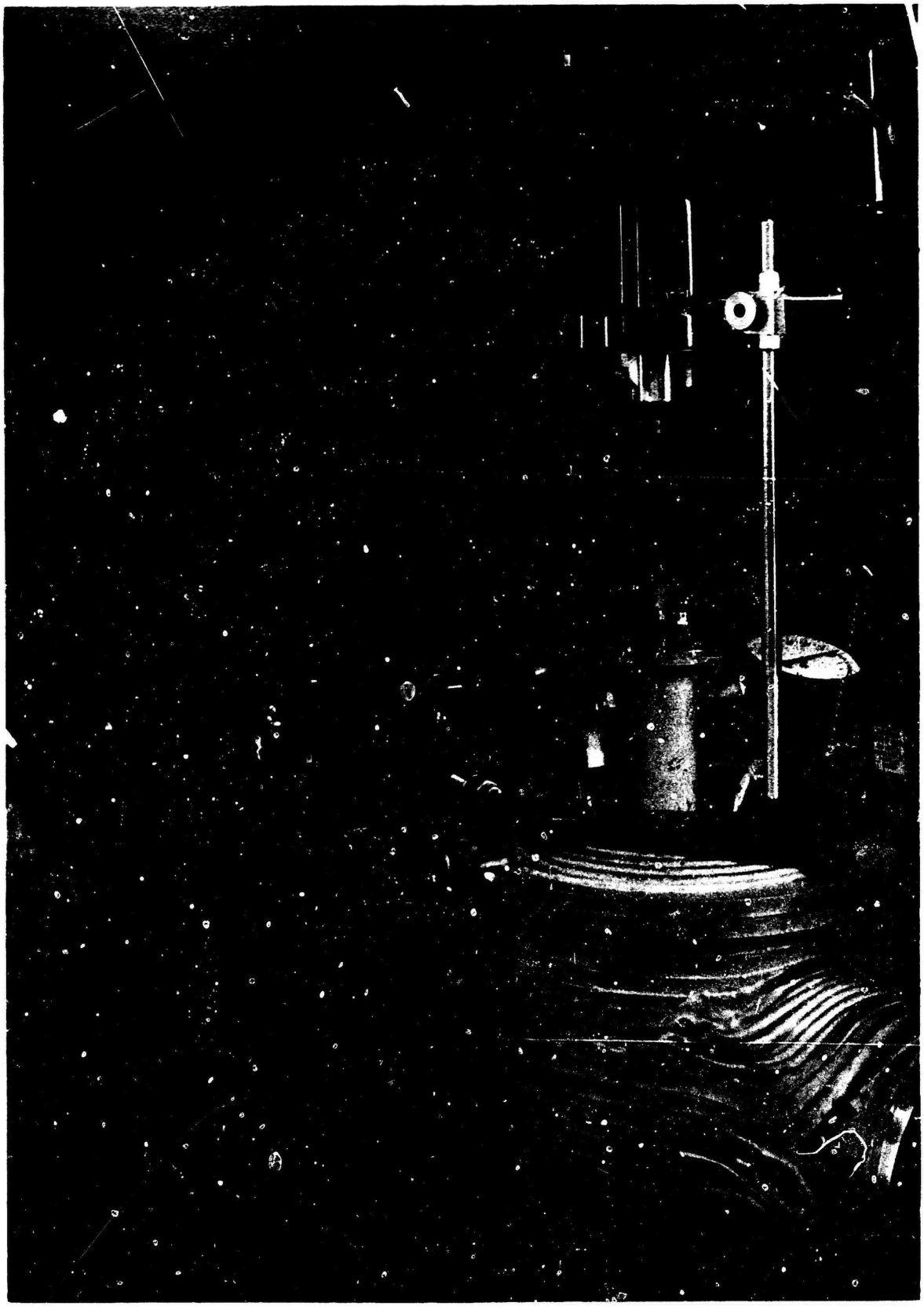

FIG. 7

VISCOSITY – TEMPERATURE CURVE FOR BARRE GRANITE

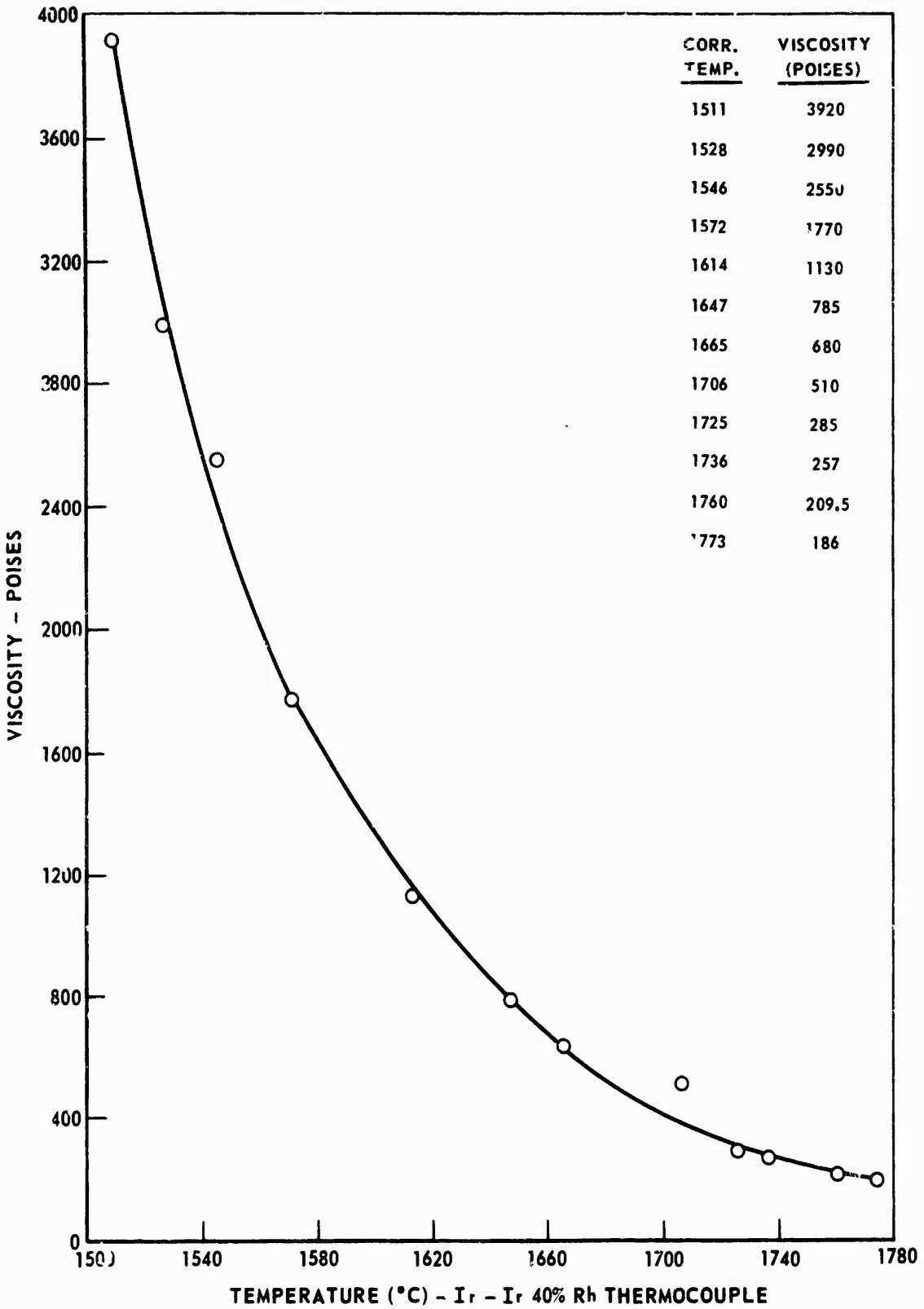

CORR. TEMP.	VISCOSITY (POISES)
1511	3920
1528	2990
1546	2550
1572	1770
1614	1130
1647	785
1665	680
1706	510
1725	285
1736	257
1760	209.5
1773	186

FIG. 8

VISCOSITY – TEMPERATURE CURVE FOR WESTERLY GRANITE

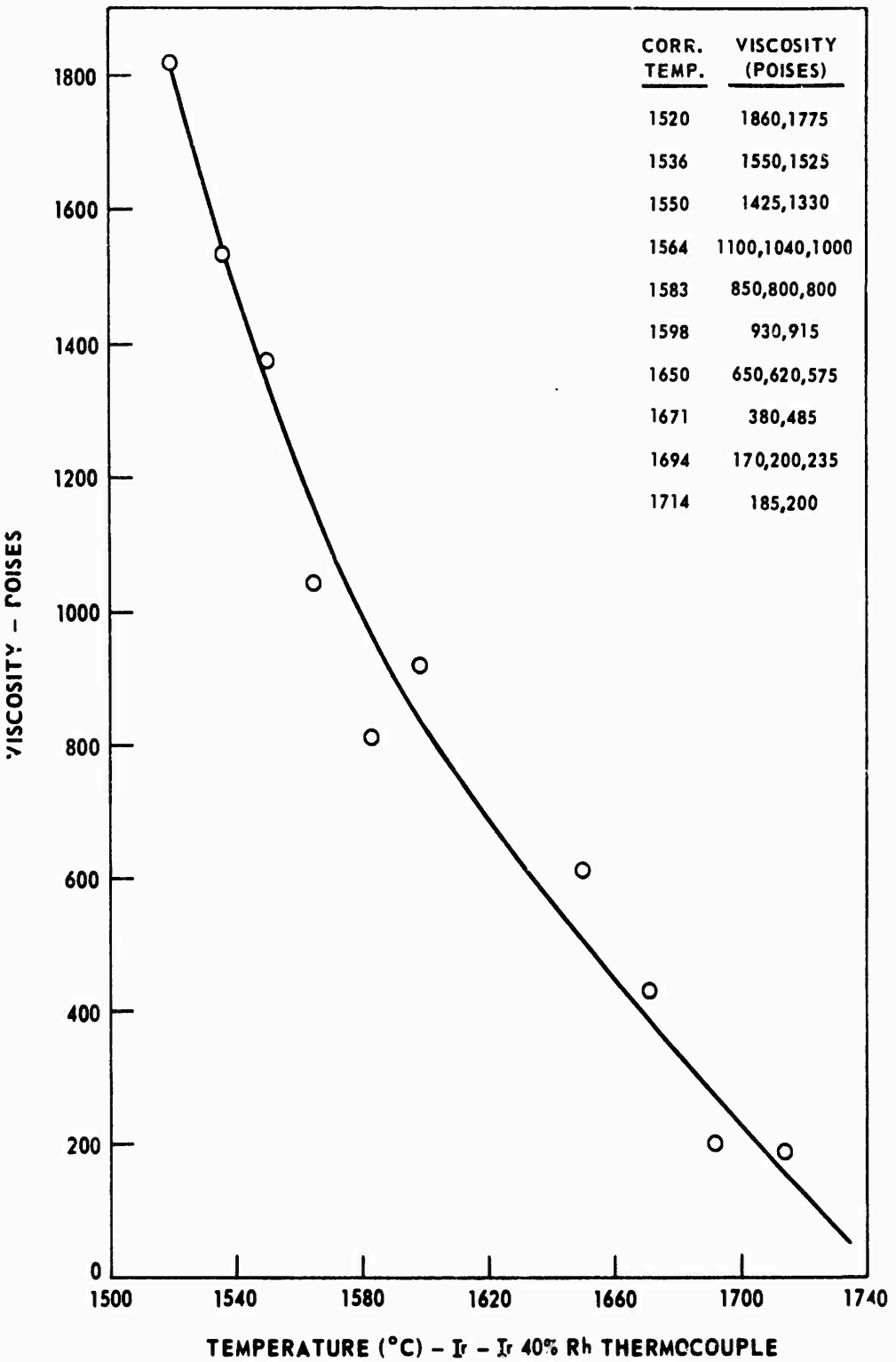

FIG. 9

VISCOSITY–TEMPERATURE CURVE FOR DULUTH GABBRO

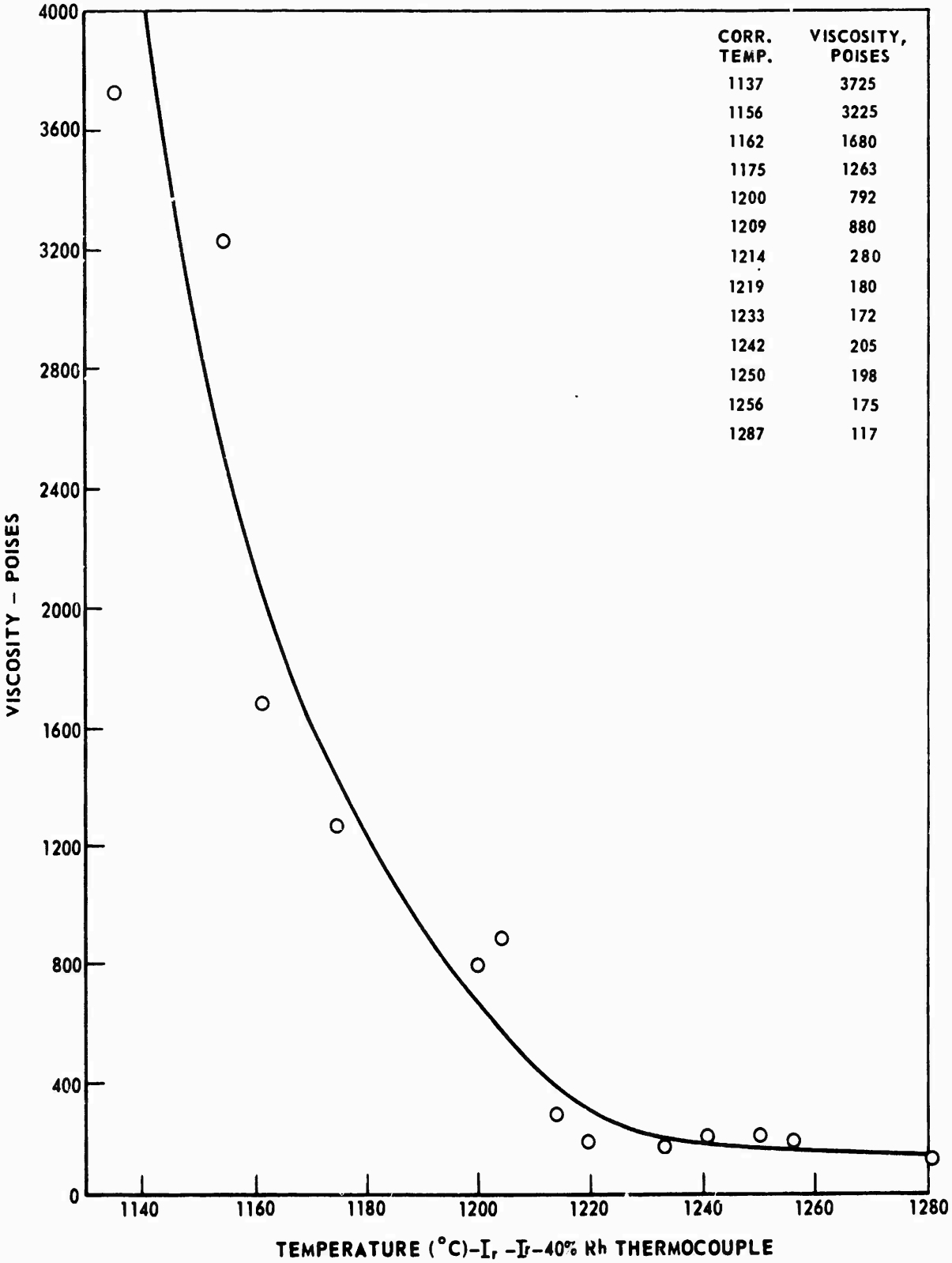

CORR. TEMP.	VISCOSITY, POISES
1137	3725
1156	3225
1162	1680
1175	1263
1200	792
1209	880
1214	280
1219	180
1233	172
1242	205
1250	198
1256	175
1287	117

L911397–4

FIG. 10

VISCOSITY – TEMPERATURE CURVE FOR CHARCOAL GRANITE

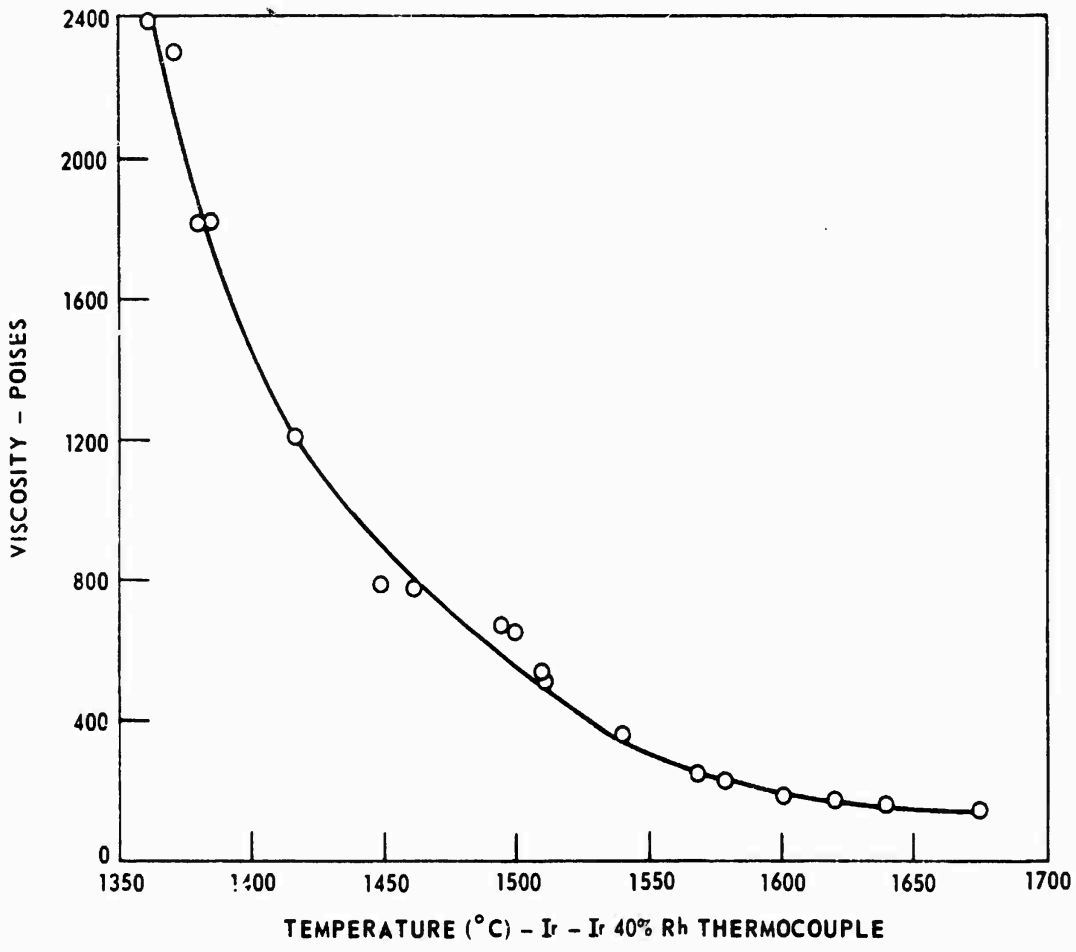

CORR. TEMP.	VISCOSITY (POISES)
1359	2396
1361	2325,2275
1380	1875,1780
1388	1875,1800
1417	1250,1275,1130,1220
1449	785,800
1461	775,790
1494	675
1497	675,625
1511	580,500
1514	570,440
1540	340,375,383
1569	250,250,256
1579	230,225,230
1606	183,192
1621	175,175,174
1639	165,165,161
1674	145,145,140,144.5,145

FIG. 11

VISCOSITY–TEMPERATURE CURVE FOR GRANODIORITE–LUNAR

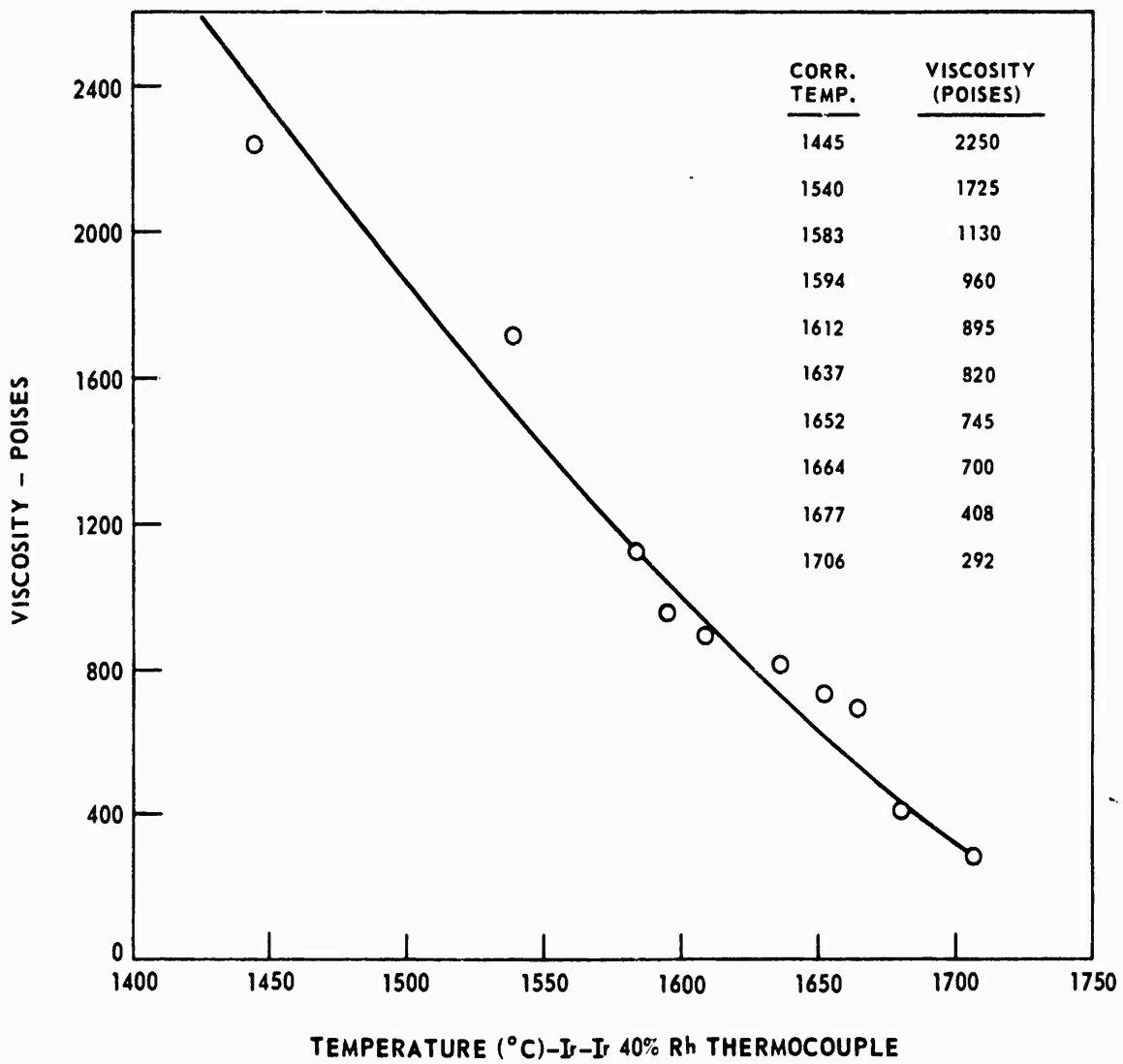

FIG. 12

VISCOSITY–TEMPERATURE CURVE FOR THOLEIITIC BASALT

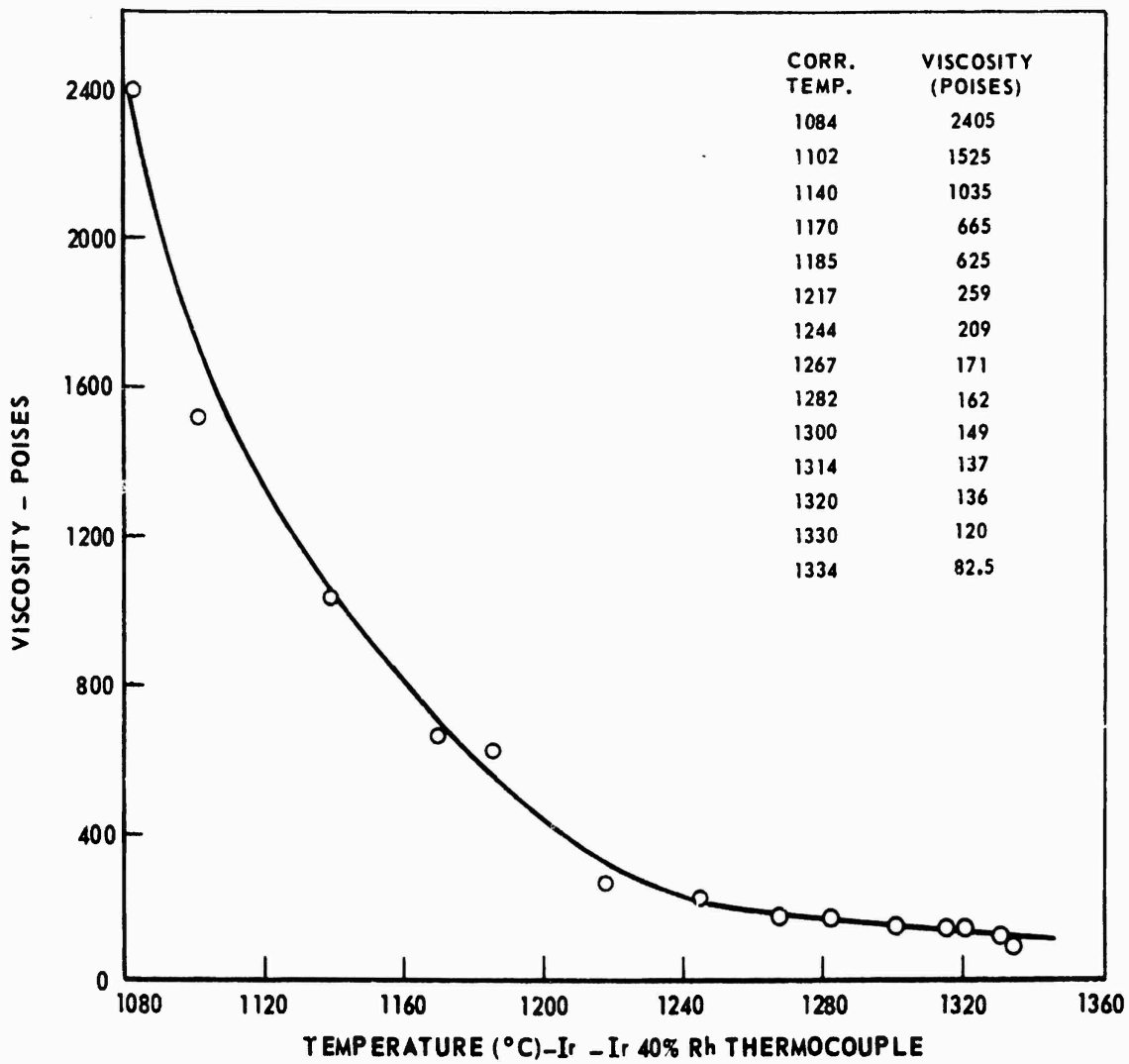

FIG. 13

VISCOSITY–TEMPERATURE CURVE FOR NEWBERRY RHYOLITE (FRESH)

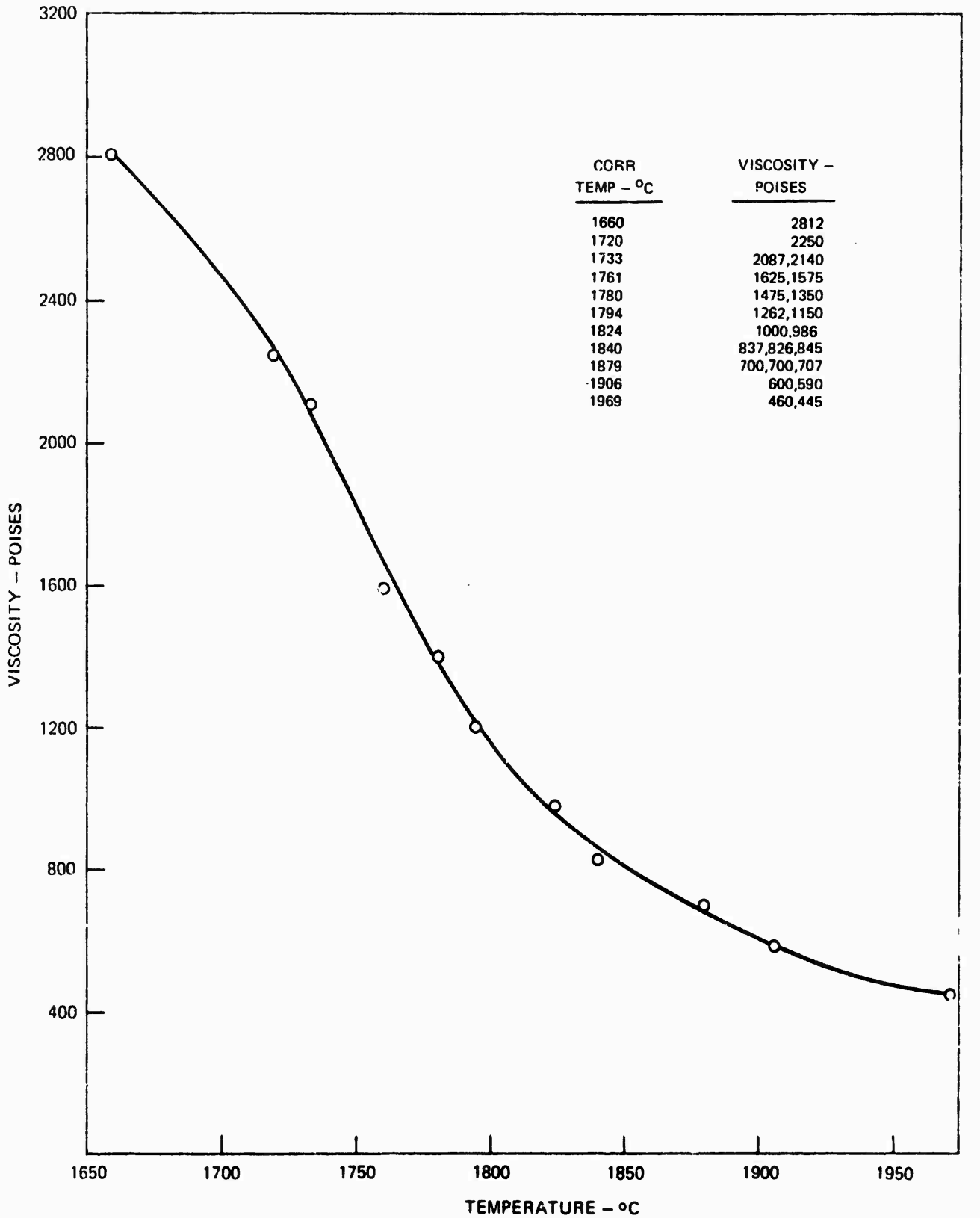

CORR TEMP – °C	VISCOSITY – POISES
1660	2812
1720	2250
1733	2087,2140
1761	1625,1575
1780	1475,1350
1794	1262,1150
1824	1000,986
1840	837,826,845
1879	700,700,707
1906	600,590
1969	460,445

FIG. 14

VISCOSITY–TEMPERATURE CURVE FOR DRESSER BASALT

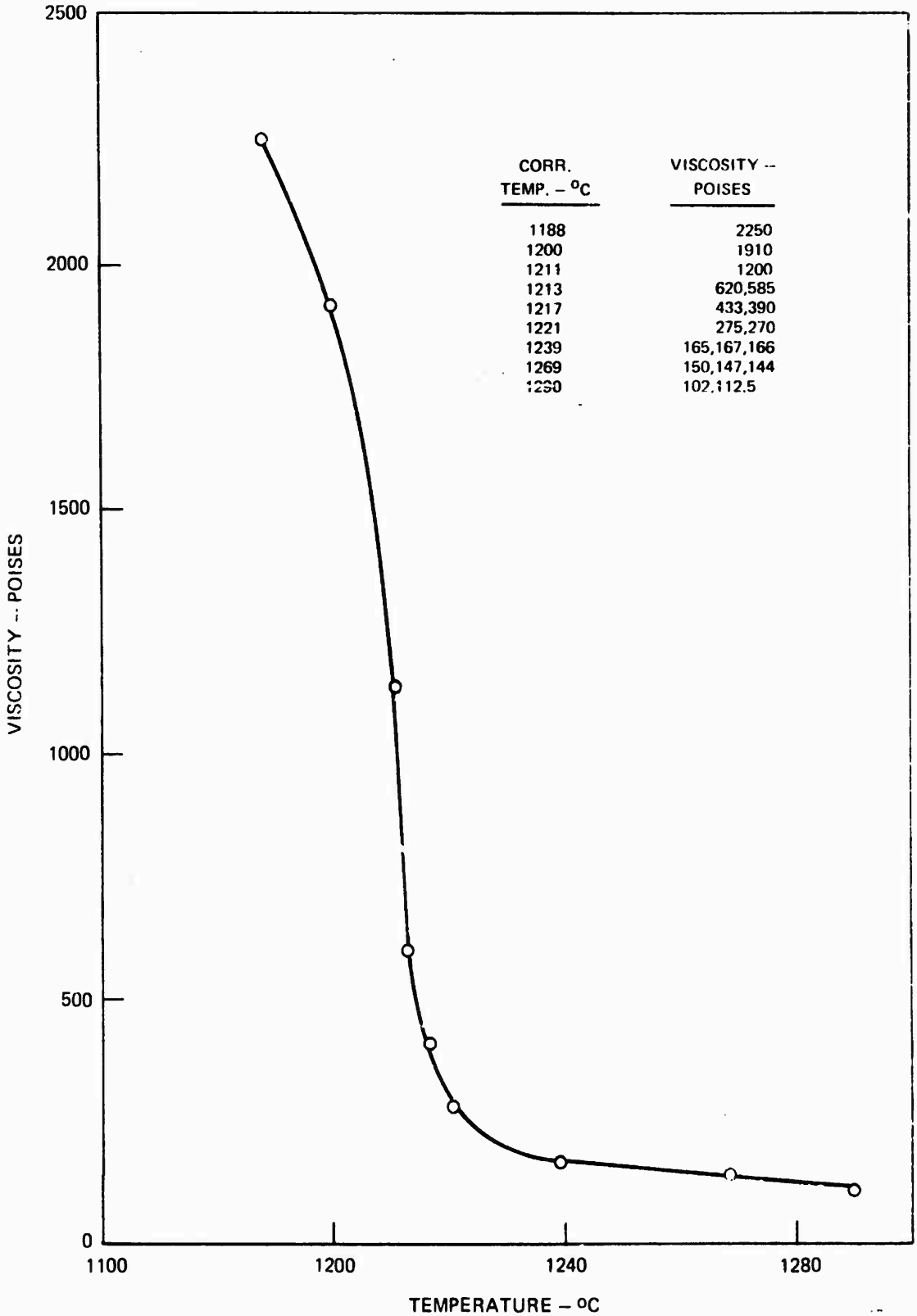

CORR. TEMP. – °C	VISCOSITY -- POISES
1188	2250
1200	1910
1211	1200
1213	620,585
1217	433,390
1221	275,270
1239	165,167,166
1269	150,147,144
1280	102,112.5

VISCOSITY – TEMPERATURE CURVE FOR BEREA SANDSTONE

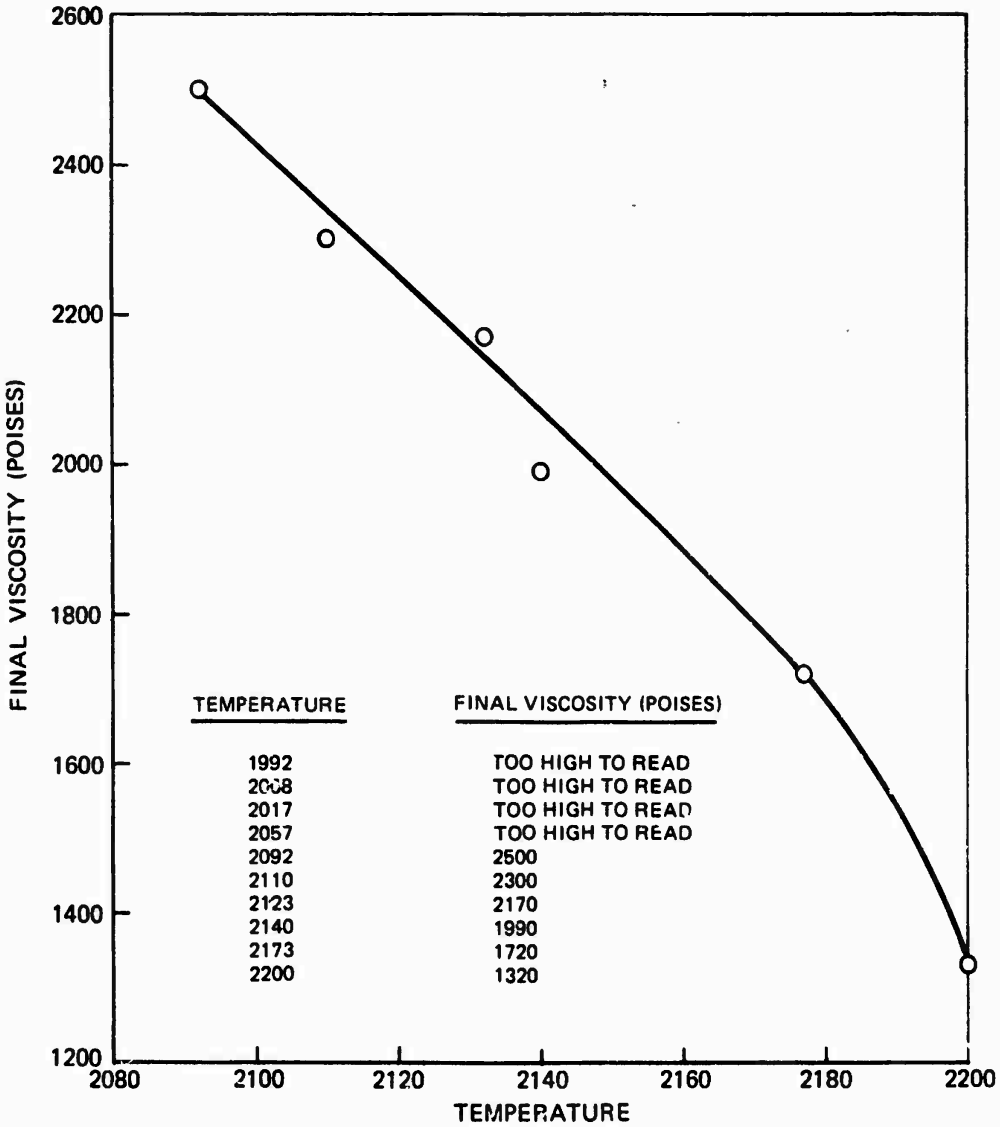

L911397–4

FIG. 16

SPECIFIC RESISTIVITY OF MOLTEN BARRE GRANITE AT HIGH TEMPERATURES

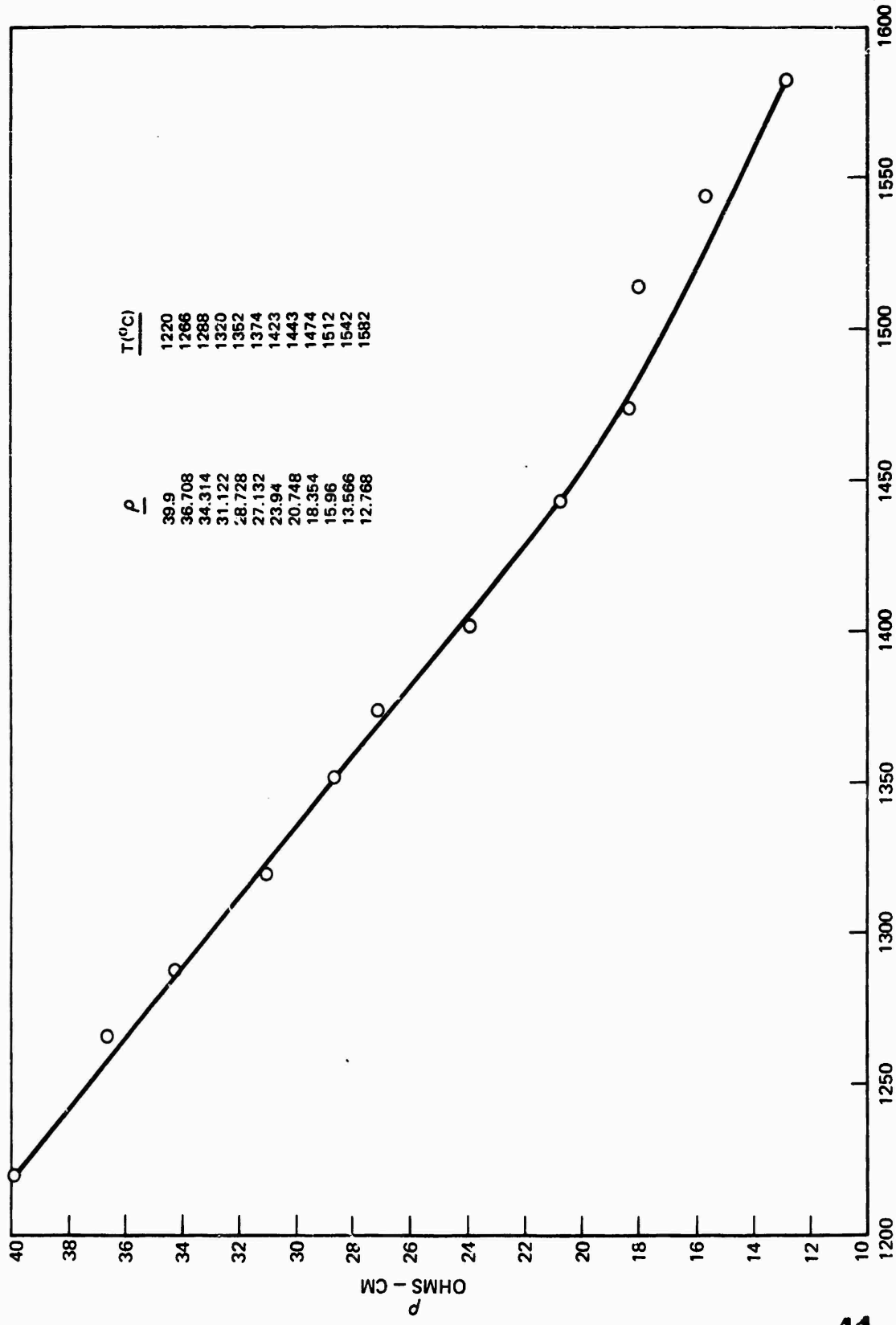

L911397–4

FIG. 17

SPECIFIC RESISTIVITY OF MOLTEN WESTERLY GRANITE AT HIGH TEMPERATURES

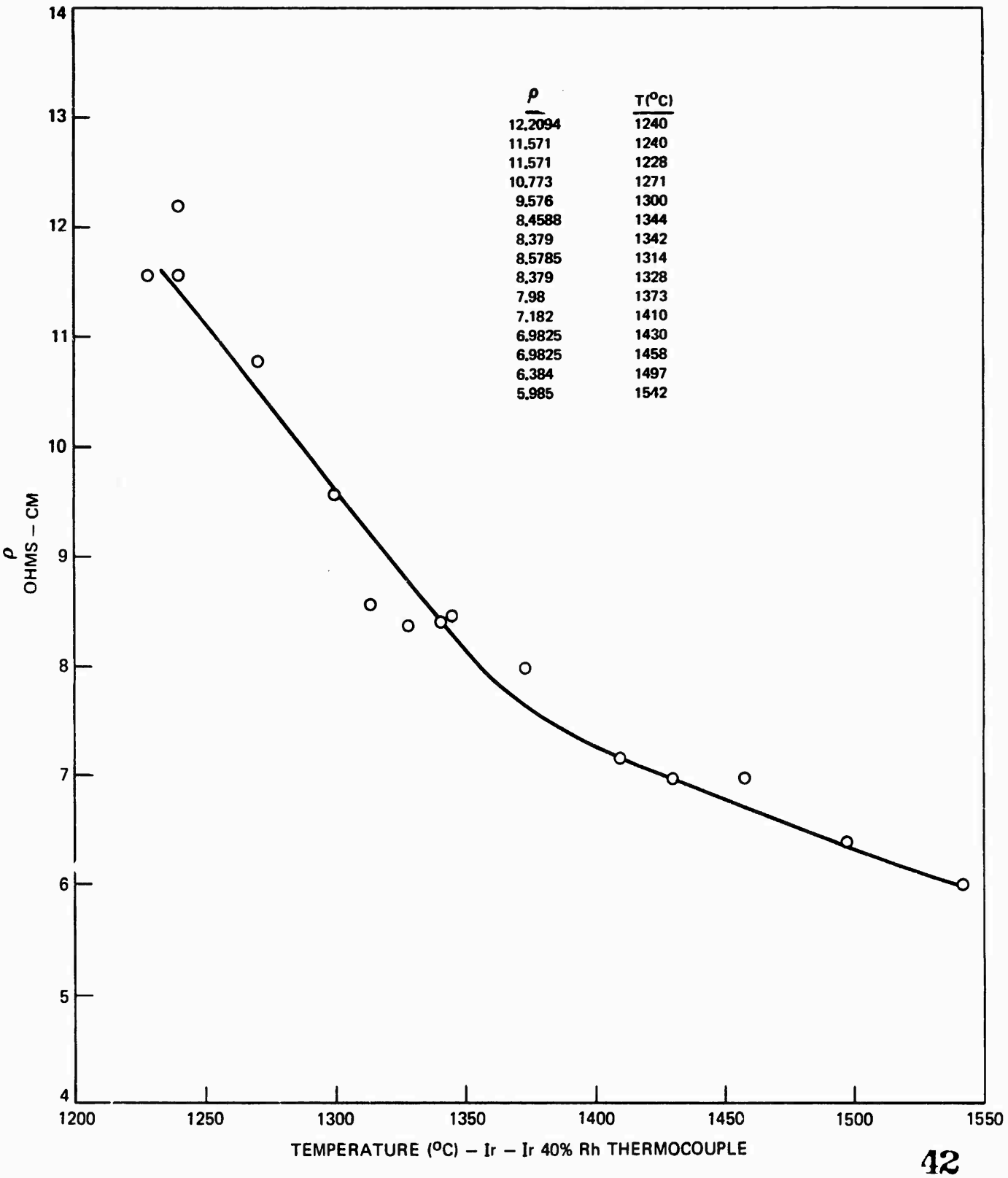

ρ	T(°C)
12.2094	1240
11.571	1240
11.571	1228
10.773	1271
9.576	1300
8.4588	1344
8.379	1342
8.5785	1314
8.379	1328
7.98	1373
7.182	1410
6.9825	1430
6.9825	1458
6.384	1497
5.985	1542

SPECIFIC RESISITIVITY OF MOLTEN DULUTH GABBRO AT HIGH TEMPERATURES

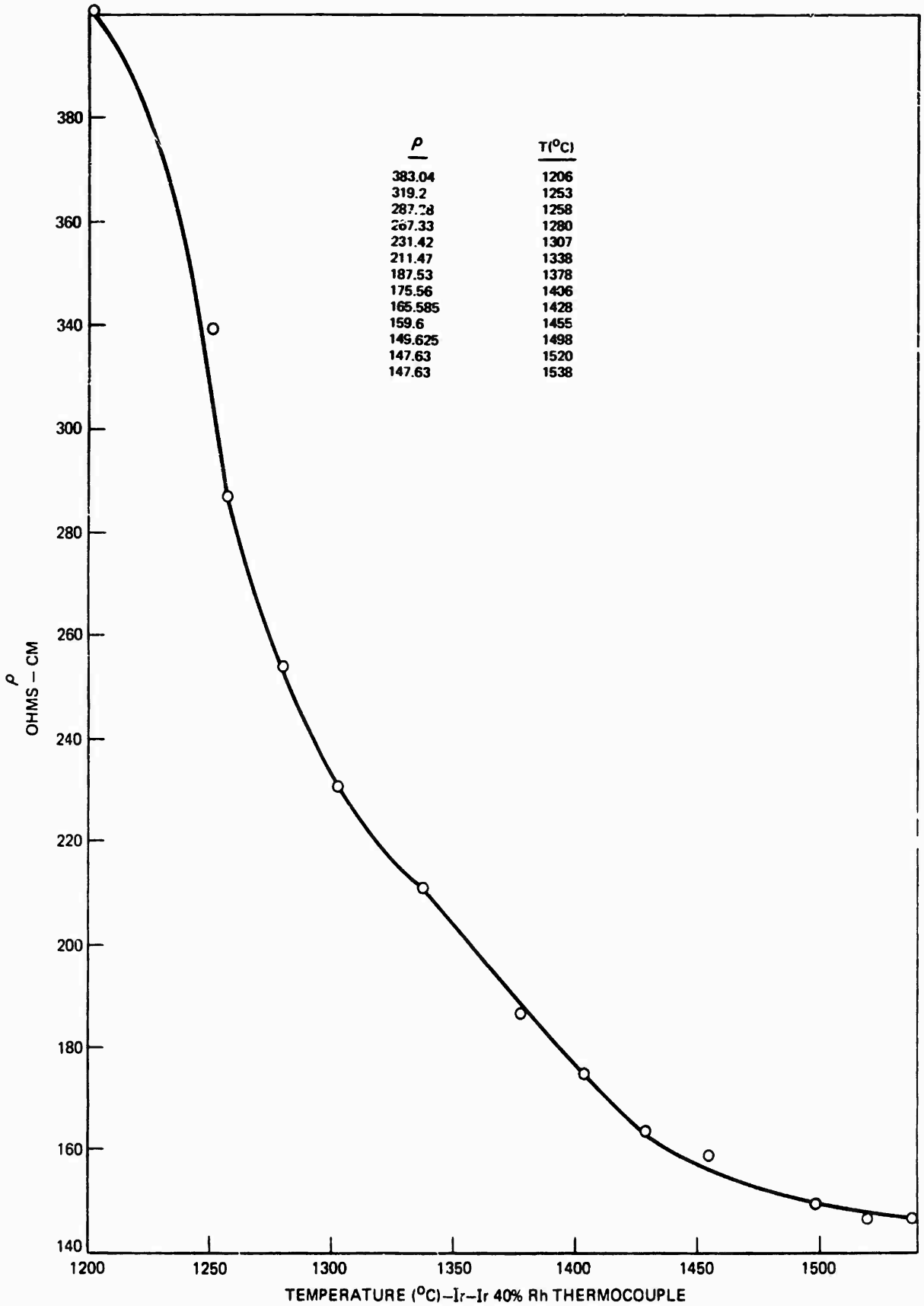

ρ	T(°C)
383.04	1206
319.2	1253
287.28	1258
267.33	1280
231.42	1307
211.47	1338
187.53	1378
175.56	1406
165.585	1428
159.6	1455
149.625	1498
147.63	1520
147.63	1538

SPECIFIC RESISITIVITY OF MOLTEN CHARCOAL GRANITE AT HIGH TEMPERATURES

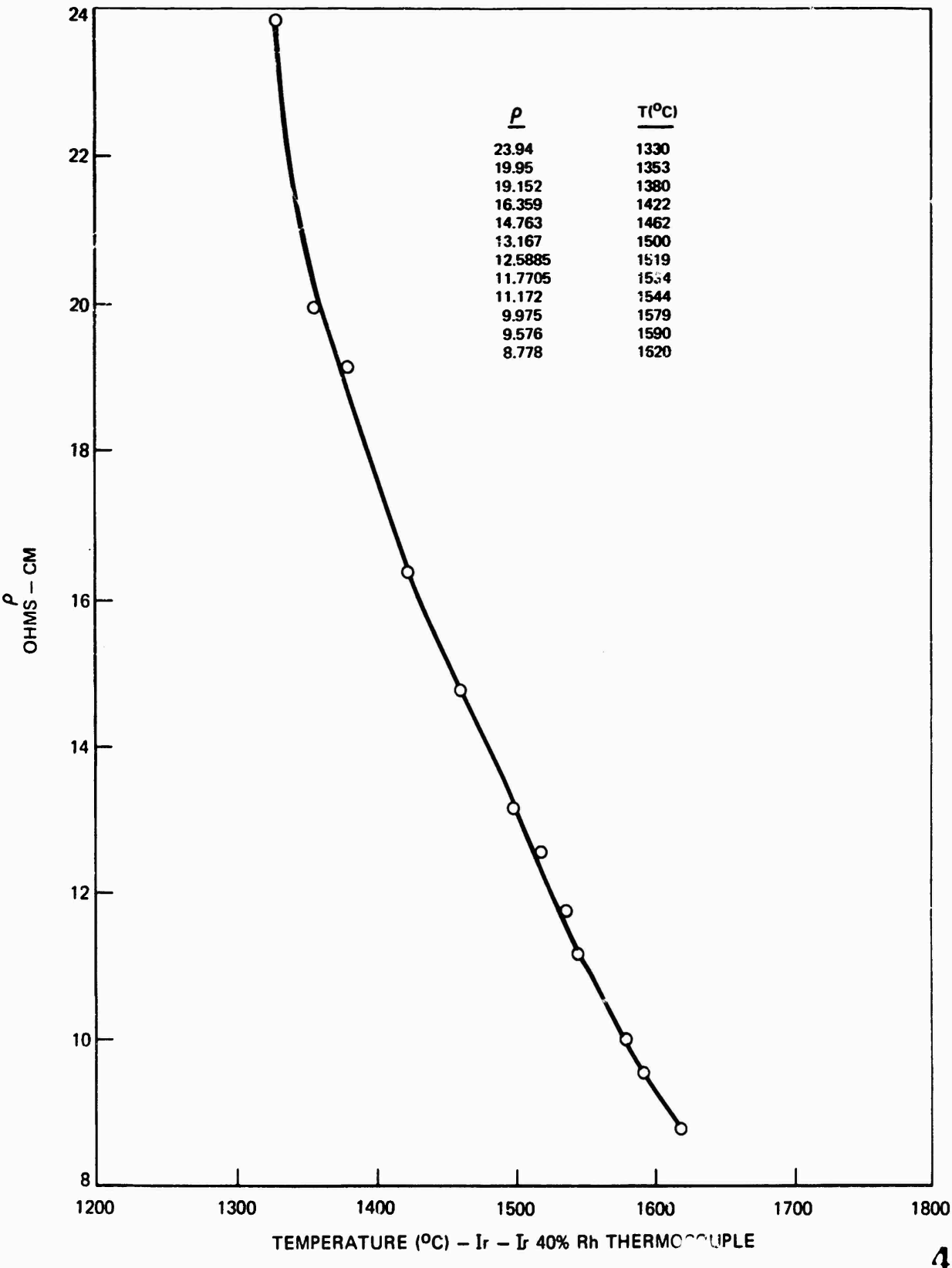

ρ	T(°C)
23.94	1330
19.95	1353
19.152	1380
16.359	1422
14.763	1462
13.167	1500
12.5885	1519
11.7705	1534
11.172	1544
9.975	1579
9.576	1590
8.778	1620

SPECIFIC RESISITIVITY OF MOLTEN GRANODIORITE–LUNAR AT HIGH TEMPERATURES

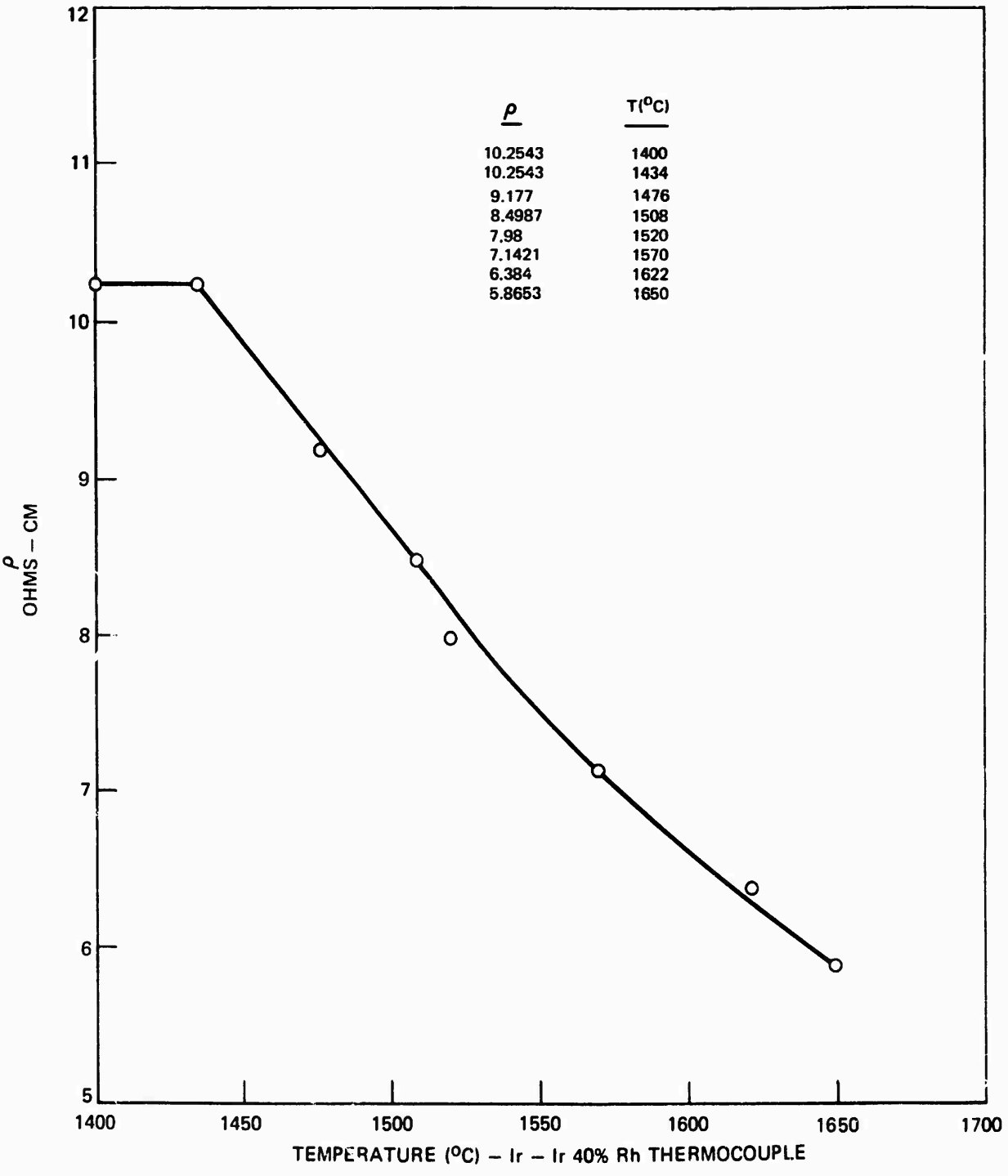

SPECIFIC RESISITIVITY OF MOLTEN THOLEIITIC BASALT AT HIGH TEMPERATURES

ρ	T(°C)
11.97	1239
8.778	1264
7.182	1308
5.586	1360
4.788	1400
4.5885	1432
3.99	1463

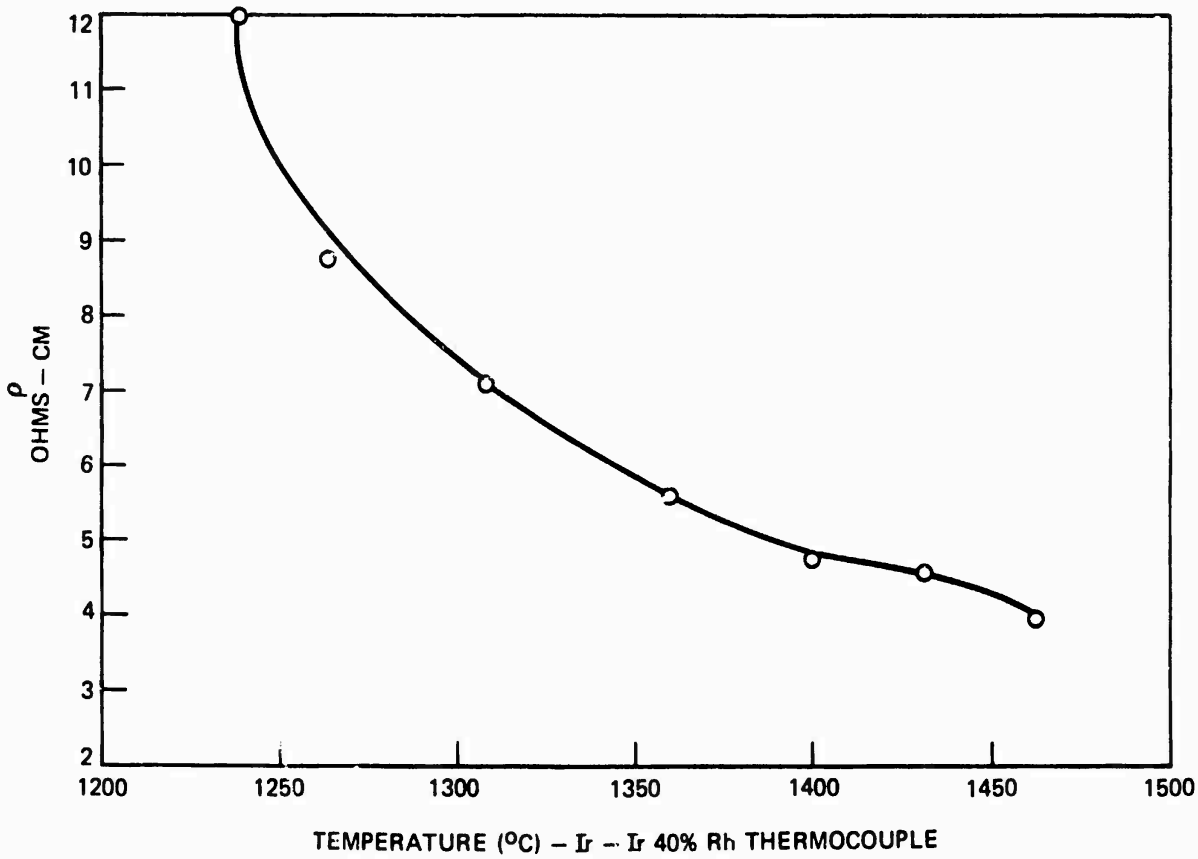

FIG. 22

SPECIFIC RESISTIVITY OF MOLTEN NEWBERRY RHYOLITE (FRESH) AT HIGH TEMPERATURES

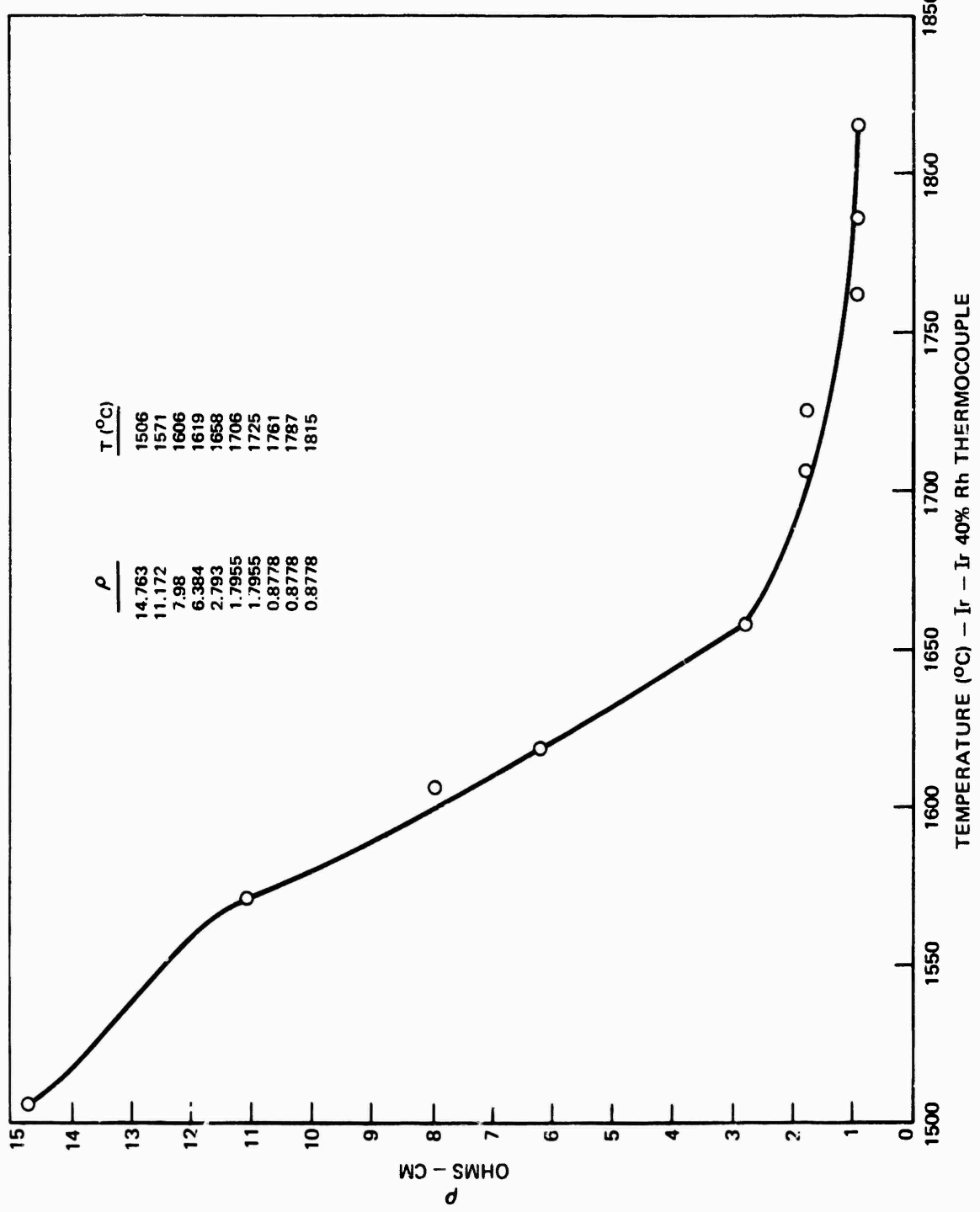

FIG. 23

SPECIFIC RESISTIVITY OF MOLTEN DRESSER BASALT AT HIGH TEMPERATURES

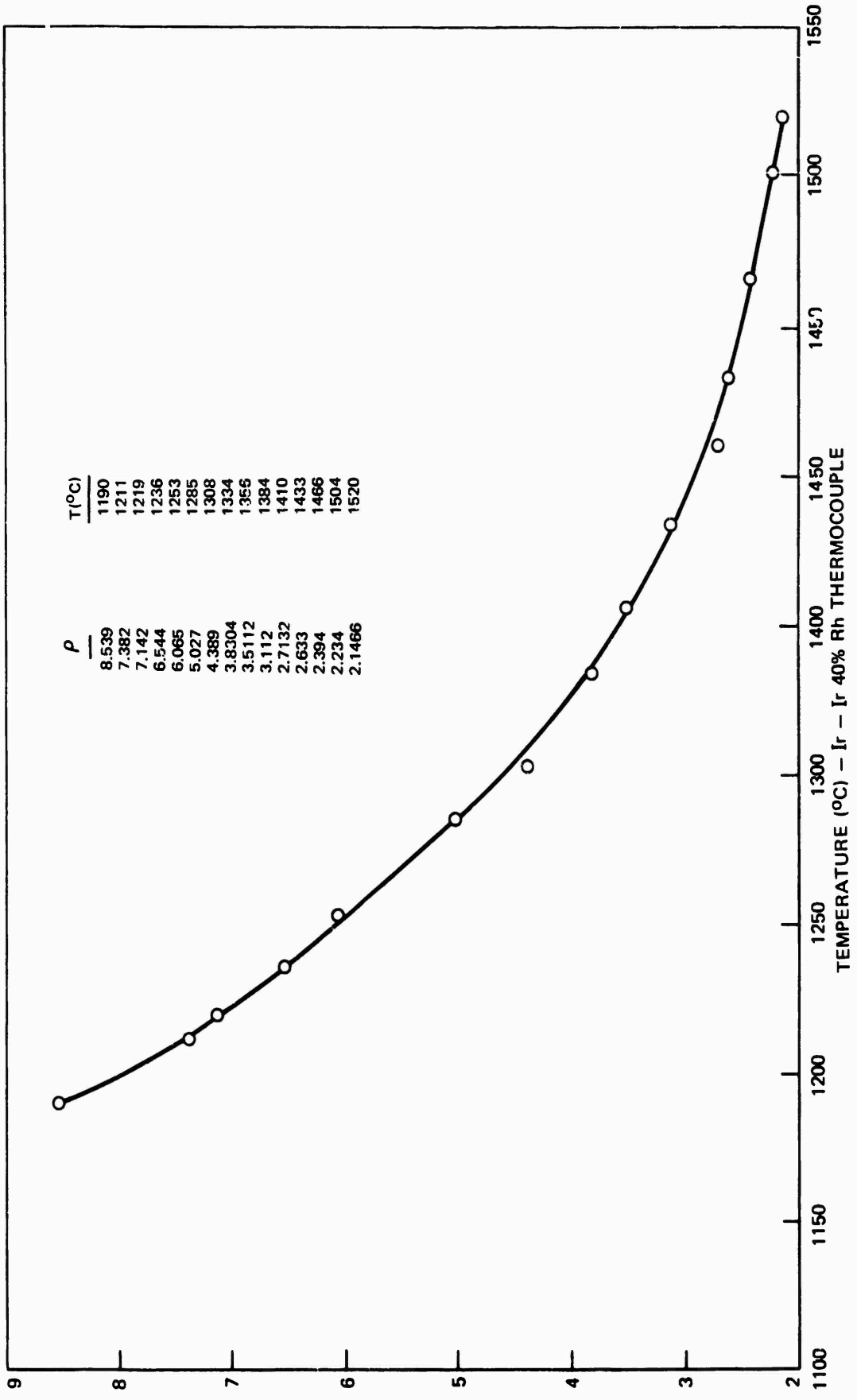

ρ	T(°C)
8.539	1190
7.382	1211
7.142	1219
6.544	1236
6.065	1253
5.027	1285
4.389	1308
3.8304	1334
3.5112	1355
3.112	1384
2.7132	1410
2.633	1433
2.394	1466
2.234	1504
2.1466	1520

FIG. 24

SPECIFIC RESISITIVITY OF MOLTEN BEREA SANDSTONE AT HIGH TEMPERATURES

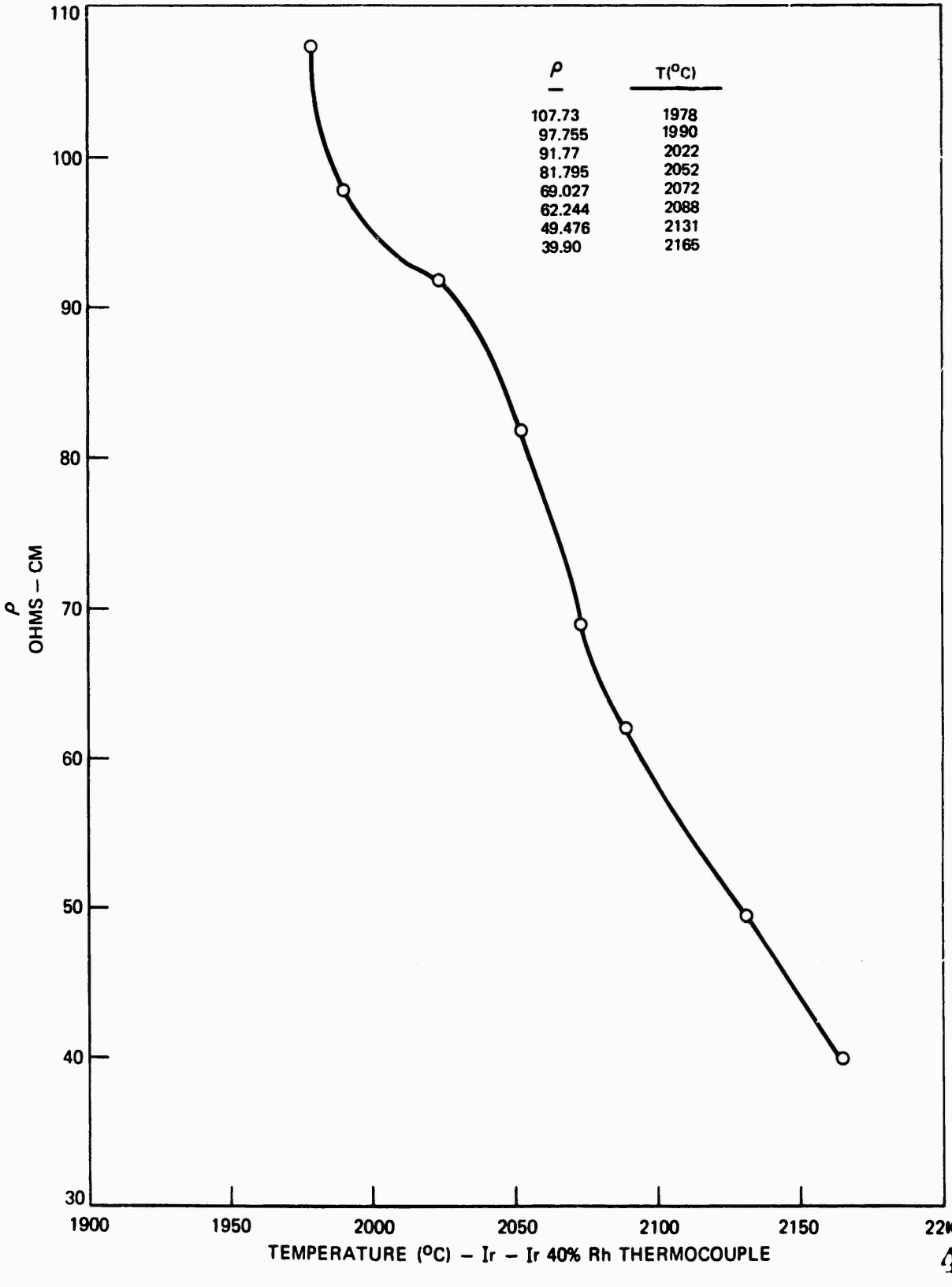

FIG. 25

LASER VAPORIZATION APPARATUS

B – LASER BEAM

P – ENTRANCE PORT

S – SAMPLE

H – SAMPLE HOLDER

M – RELEASE MECHANISM

D – DRY CALORIMETER

G – GLASS SLEEVE

E – COPPER END CAP

F – THERMOS FLASK

C – COPPER SHIELD

R – SUPPORTING COLLAR

L – COPPER LINER

A – GAS PORT

T_C – THERMOCOUPLE

ST – STIRRER

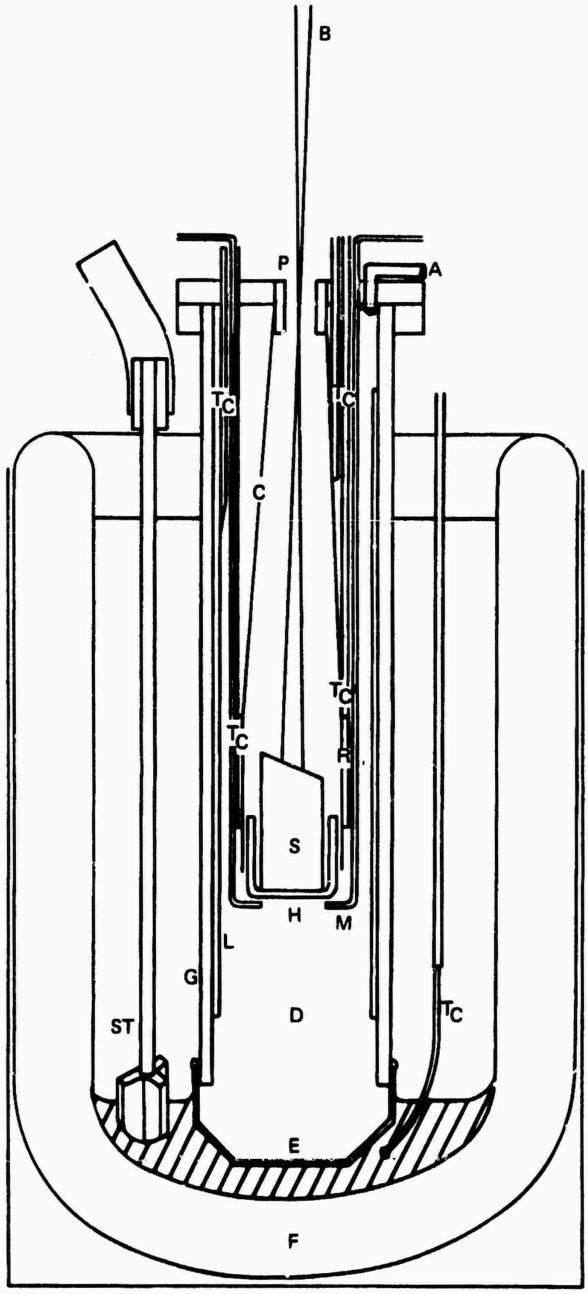

FIG. 26

ASSEMBLED APPARATUS

RL–72–374–A

FIG. 27

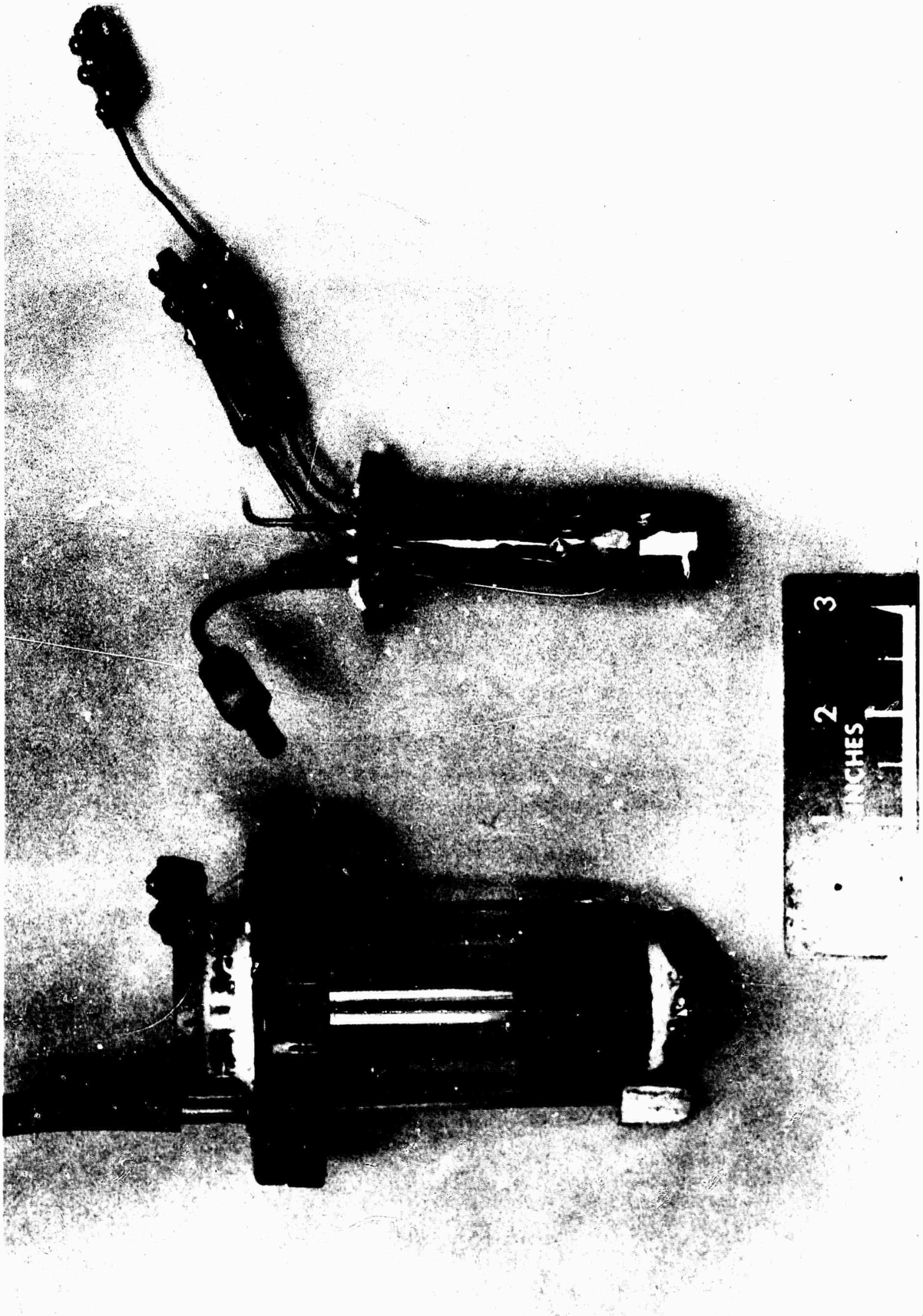

DISASSEMBLED APPARATUS

FIG. 28

REMOVABLE ELEMENTS

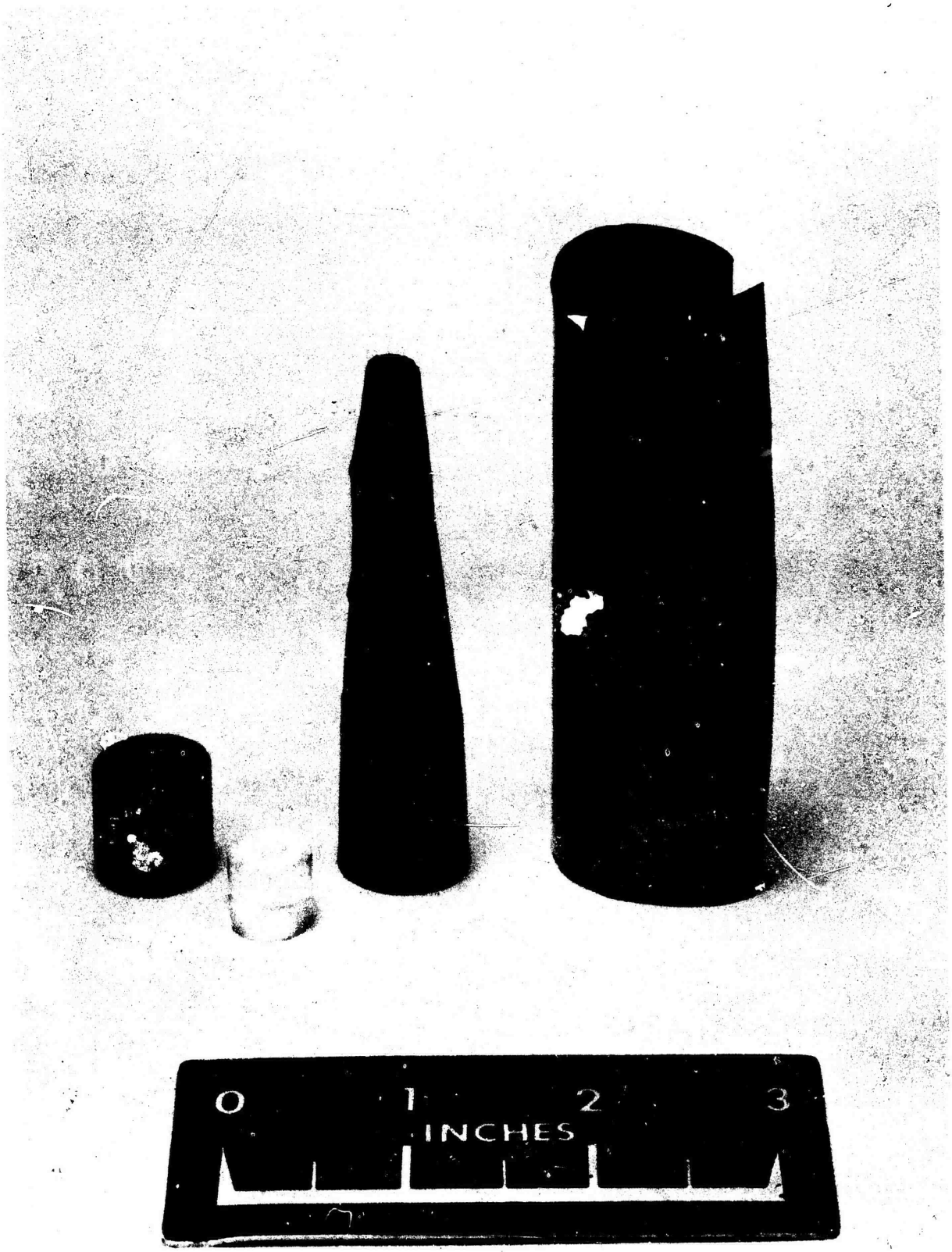

FIG. 29

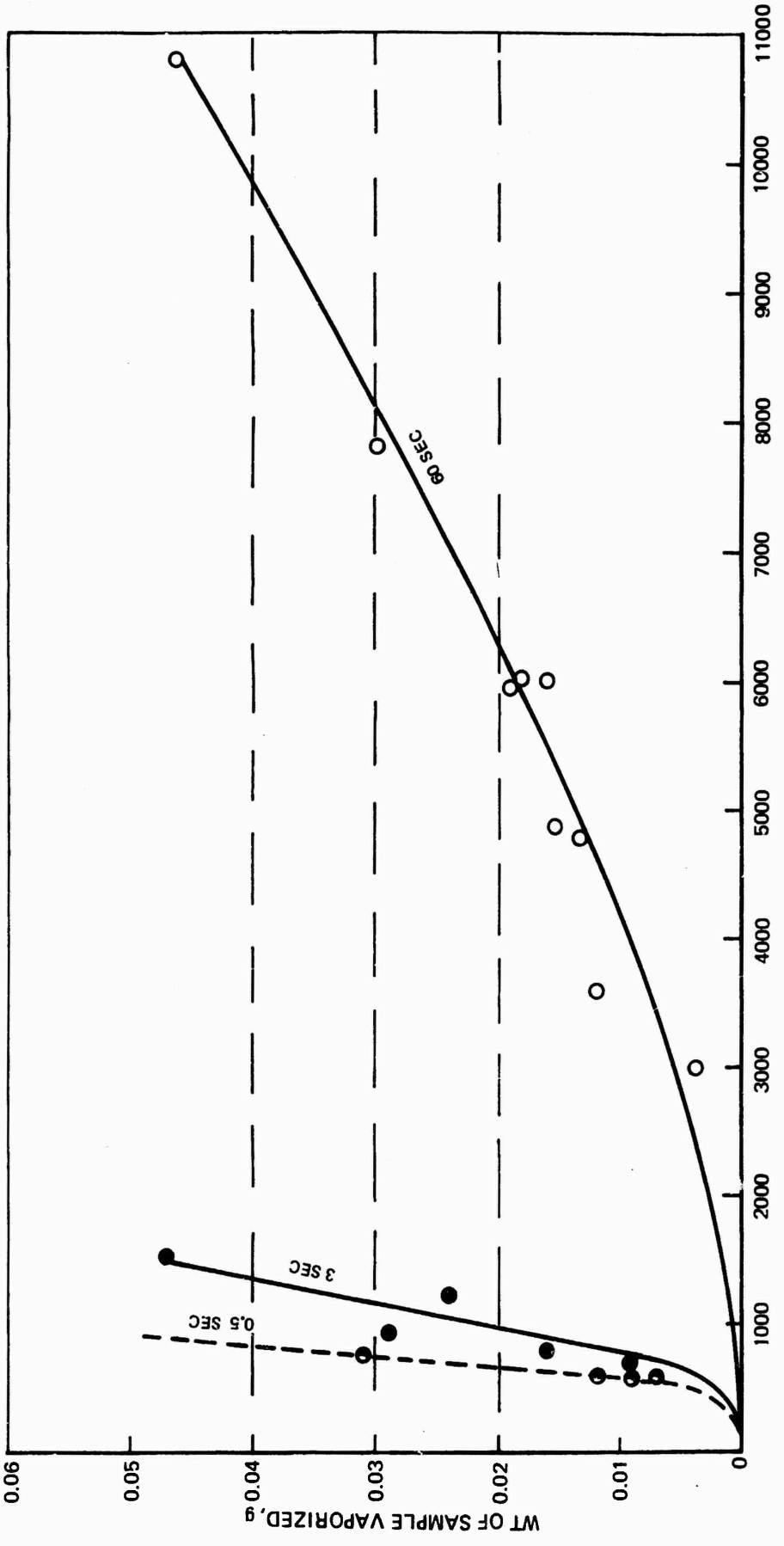
WEIGHT OF SiO_2 VAPORIZED VS LASER INPUT POWER AT VARIED RUN TIMES
WT OF SAMPLE VAPORIZED, g
0.06
0.05
0.04
0.03
0.02
0.01
0
1000
2000
3000
4000
5000
6000
7000
8000
9000
10000
11000
WATTS X SEC
60 SEC
3 SEC
0.5 SEC

WEIGHT OF SiO_2 VAPORIZED VS HEAT TO CALORIMETER FOR DIFFERENT RUN TIMES

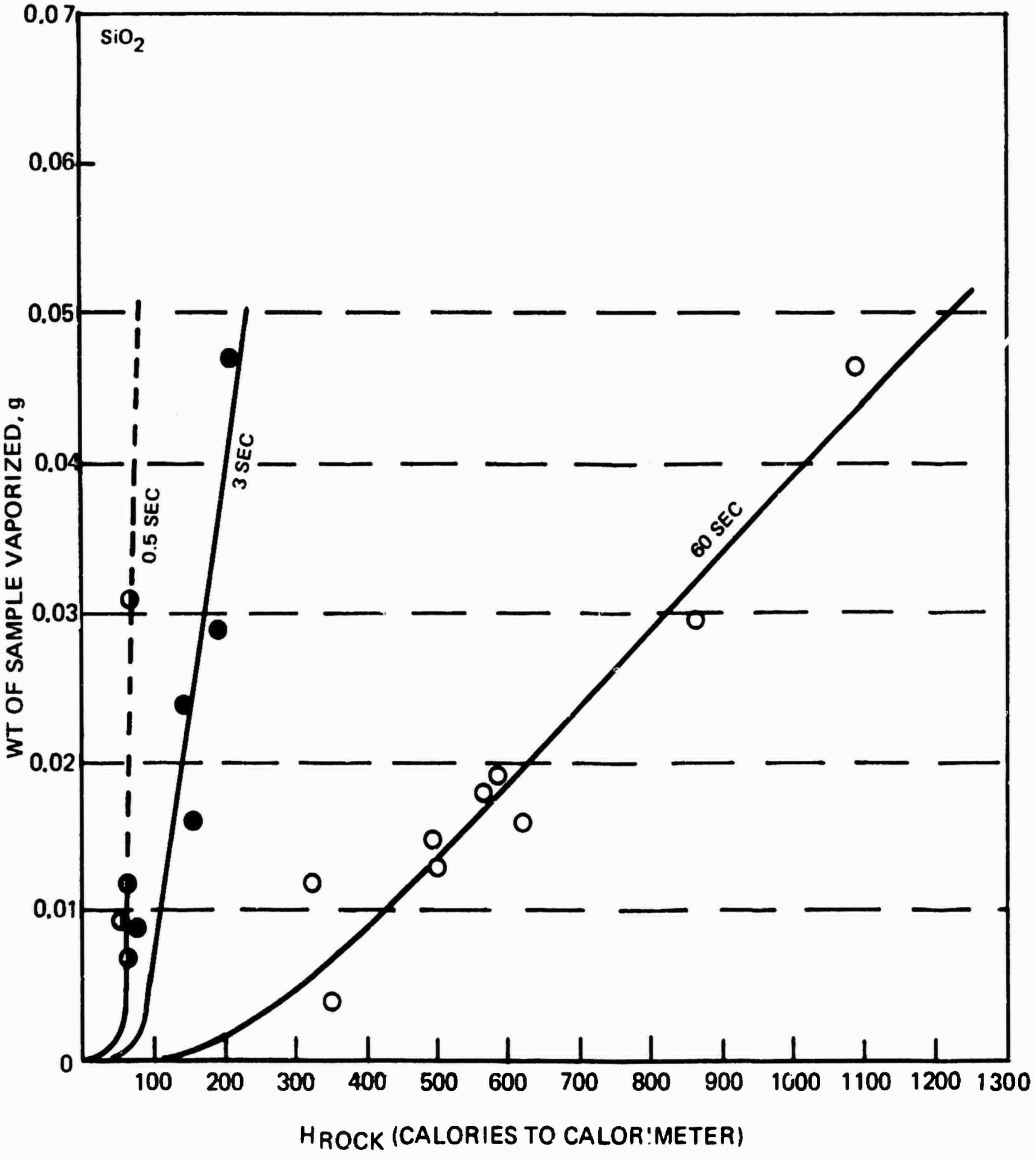

FIG. 31

FINAL TEMPERATURE OF SHIELD VERSUS LASER INPUT POWER AT VARIOUS RUN TIMES

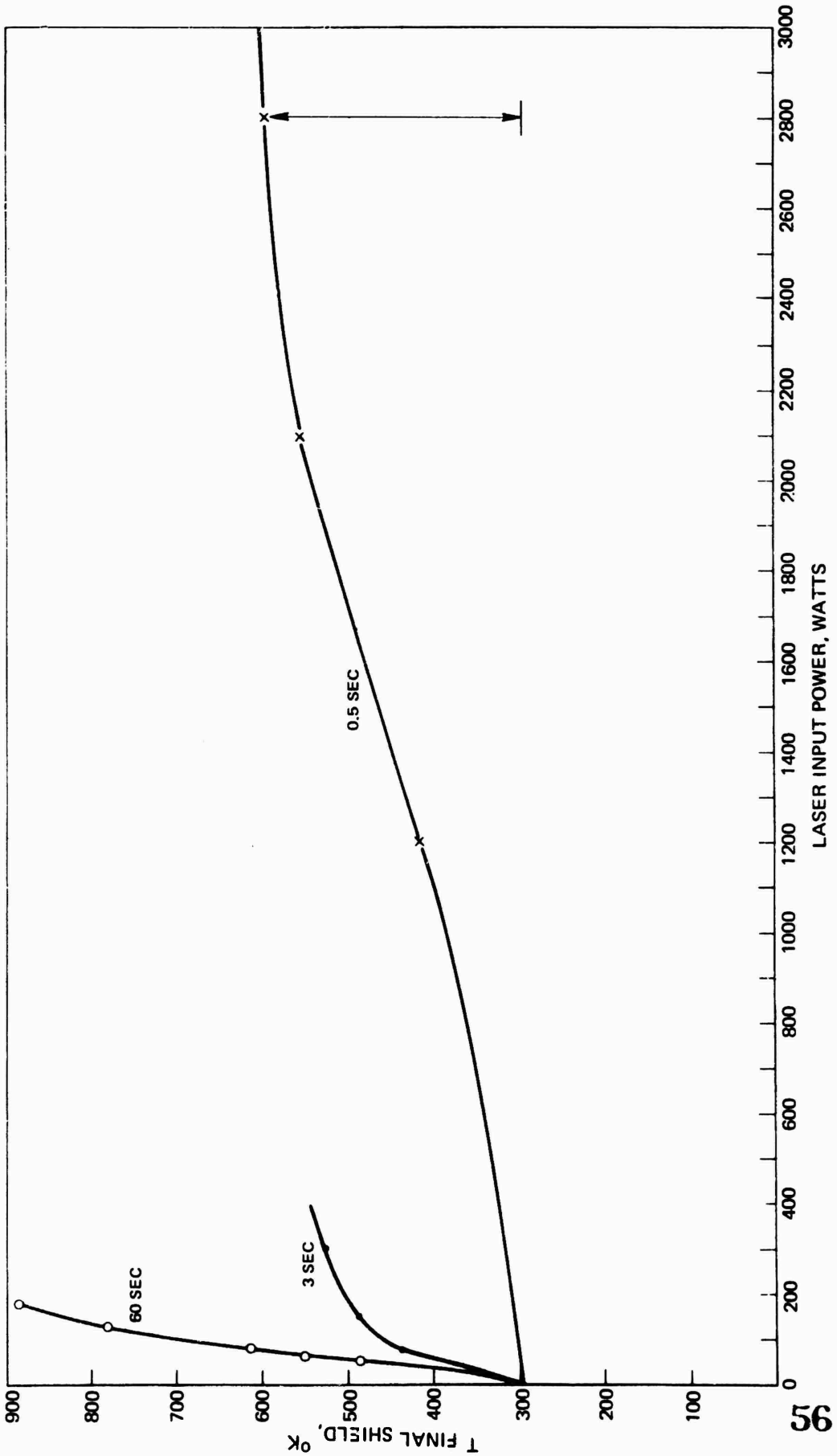

ESTIMATED TOTAL HEAT OF VAPORIZATION

$$H_{VT} = C_P \Delta T + H_f + H_V = \frac{H_{IN.} - H_{MEASURED} - H_{LOSS}}{W_V - W_C}$$

WHERE C_P = AVERAGE SPECIFIC HEAT

$\Delta T = T_{V_{UP}} - T_{ROOM}$

H_f = HEAT OF FUSION

H_V = HEAT OF VAPORIZATION

$H_{IN.}, H_{MEASURED}$ = GIVEN IN TABLE II

H_{LOSS} = 0 (ASSUMED)

W_V = WT. OF ROCK VAPORIZED

W_C = WT. OF ROCK CONDENSED ON SHIELD

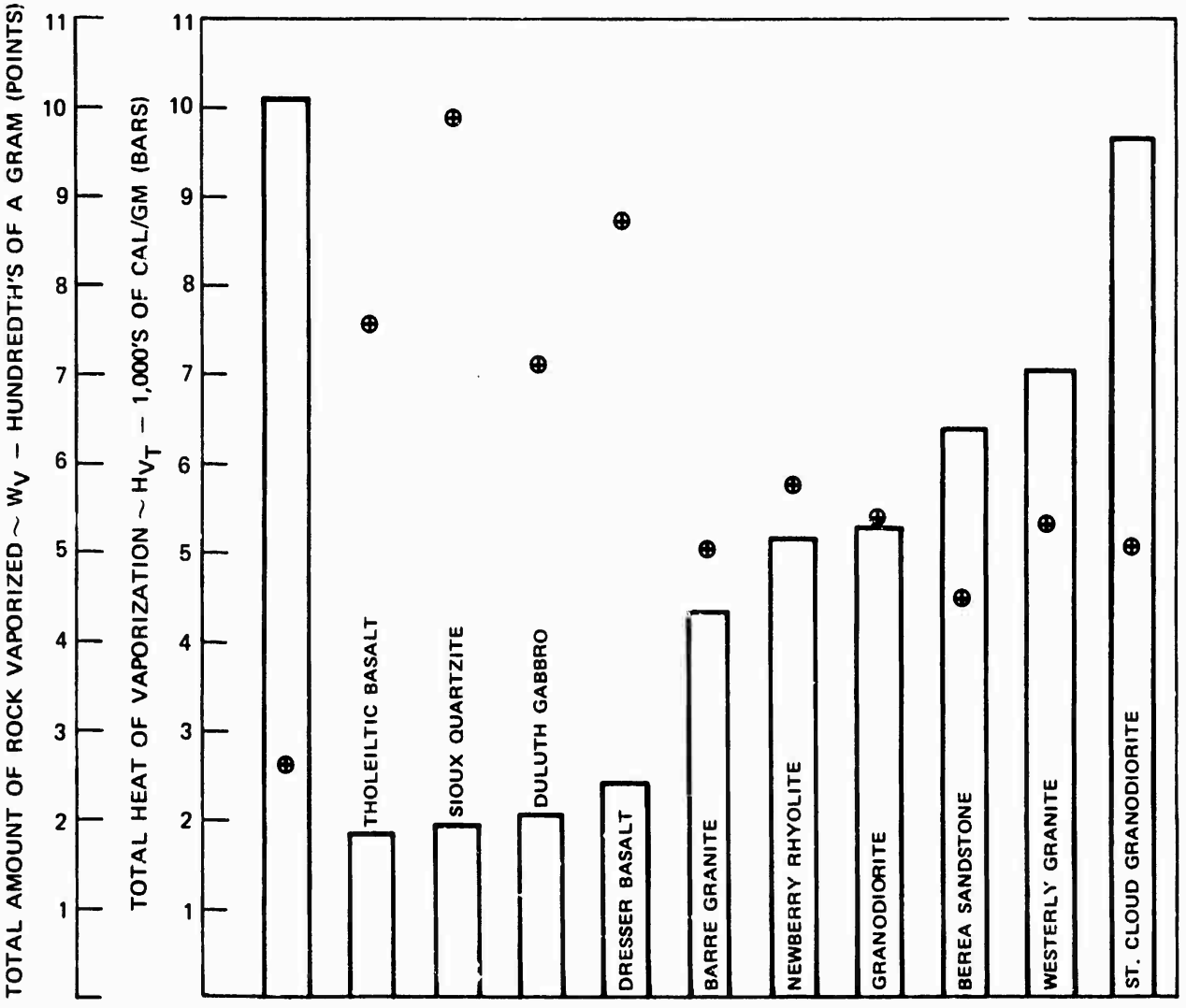

FIG. 33

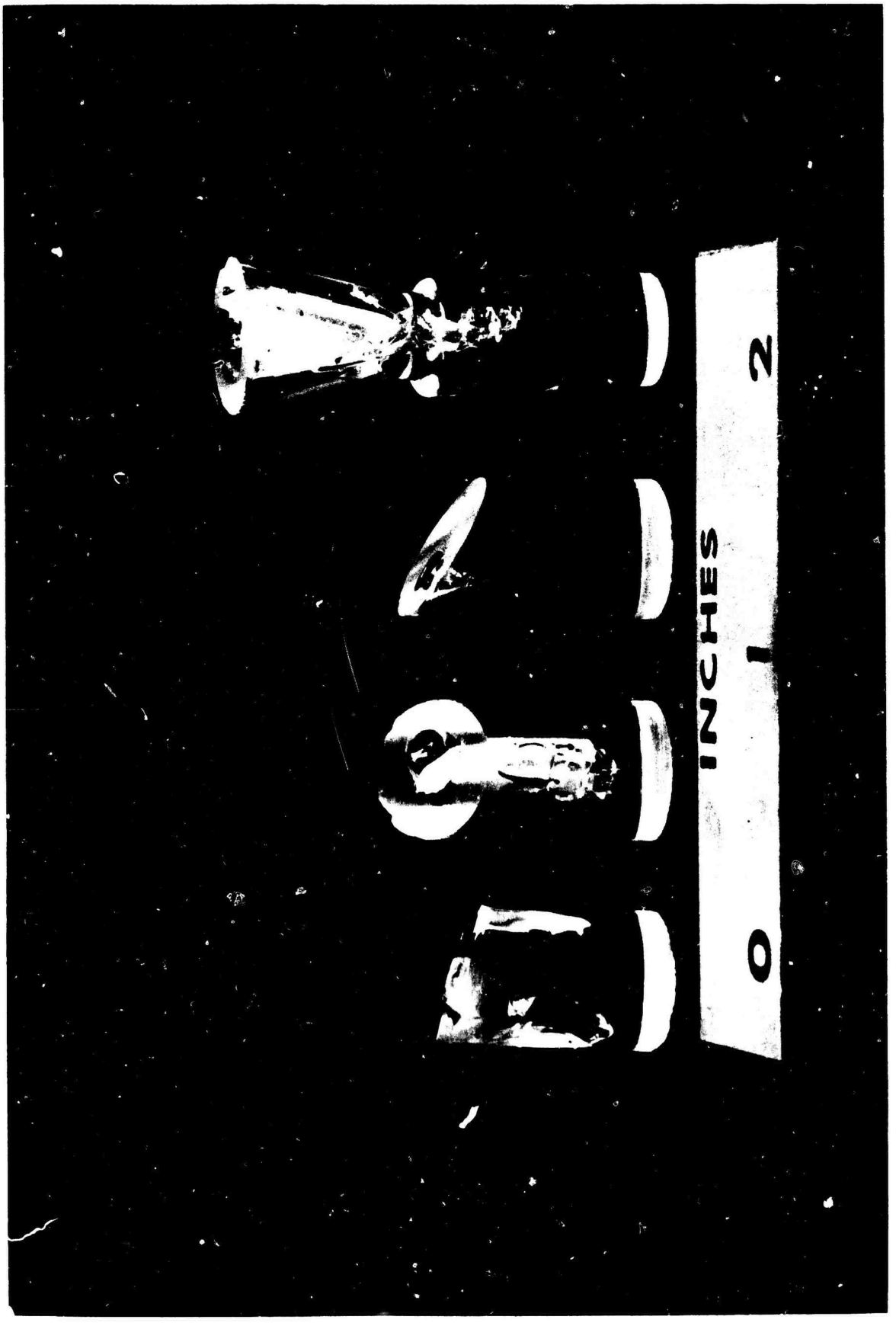

SPECIMEN SHAPES

SPECIMEN SHAPES TESTED

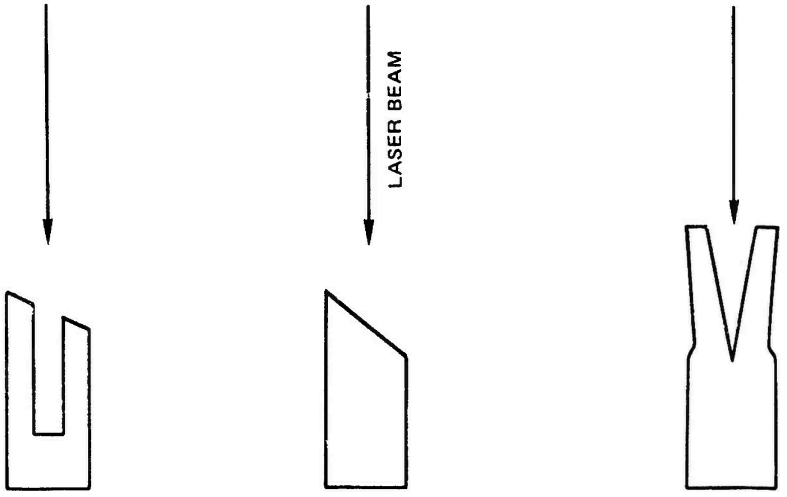

BEFORE PULSE

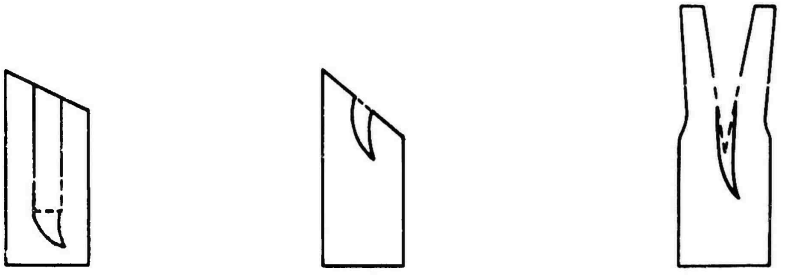

AFTER PULSE

FIG. 35

BEAM DEFLECTION VS TIME

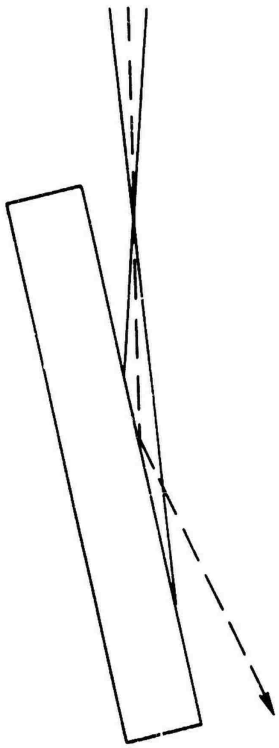

START (1)

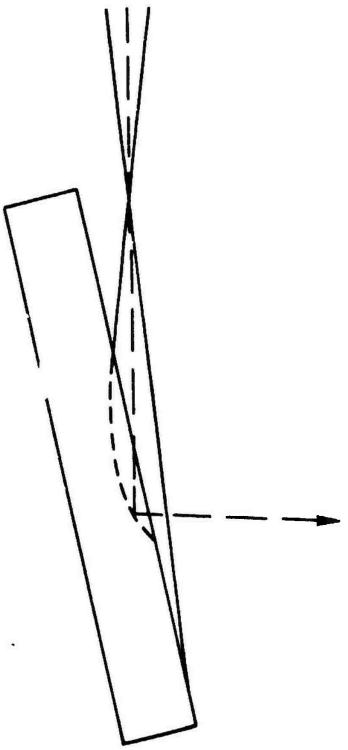

(2)

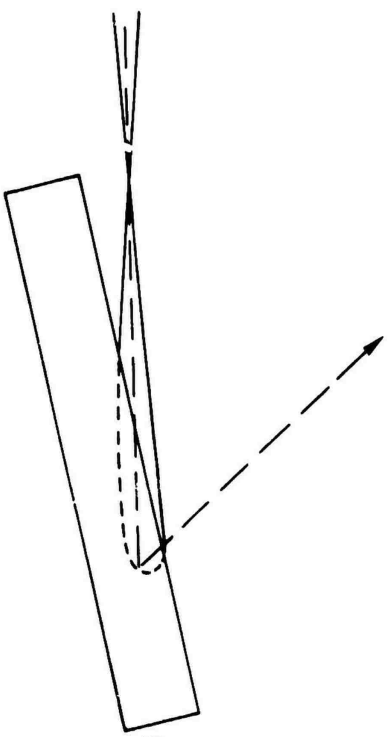

(3)

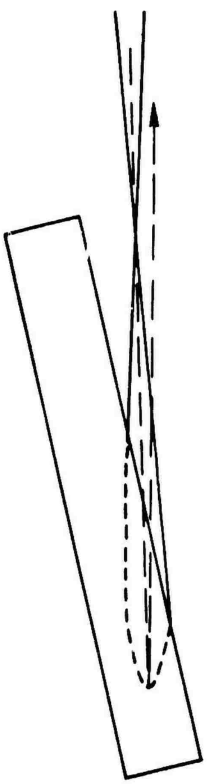

(4) STOP

FIG. 36

REVISED APPARATUS DESIGN

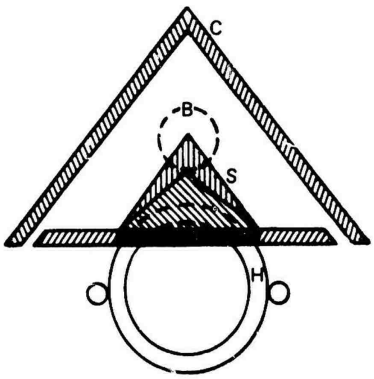

TOP VIEW OF SAMPLE,
SAMPLE HOLDER, AND SHIELD

B – LASER BEAM

S – SAMPLE

H – SAMPLE HOLDER

C – SHIELD

J – CONE CALORIMETER